Results of NRP 20

Deep structure of the Swiss Alps

Editors

O.A. Pfiffner

P. Lehner

P. Heitzmann

St. Mueller

A. Steck

Coordination

P. Heitzmann

Technical assistance and advice

W. Frei

K. Graf

H. Horstmeier

L. Levato

E. Lanz

S. Sahli

Birkhäuser Verlag
Basel · Boston · Berlin

Coordination for Editing:

Dr. Peter Heitzmann
Swiss National Hydrological and
Geological Survey
CH-3003 Bern
Switzerland

e-mail: Peter.Heitzmann@Buwal.Admin.ch

Publiziert mit Unterstützung des Schweizerischen Nationalfonds zur Förderung der wissenschaftlichen Forschung

Library of Congress Cataloging-in-Publication Data

Deep structure of the Swiss Alps : results of NRP 20 / editors, O.A. Pfiffner ... [et al.] .
p. cm.
ISBN 0-8176-5254-X (alk. paper)
1. Geology, Structural–Switzerland–Alps, Swiss. 2. Alps, Swiss (Switzerland) I. Pfiffner, Othmar Adrian, 1947– . II. NRP 20 (Switzerland)
QE633.S9D43 1997 96-51014
551.8'09494'7-dc21 CIP

Deutsche Bibliothek Cataloging-in-Publication Data

Deep structure of the Swiss Alps : results of NRP 20 / ed.:
A. O. Pfiffner ... – Basel ; Boston ; Berlin : Birkhäuser, 1997
ISBN 3-7643-5254-X (Basel ...)
ISBN 0-8176-5254-X (Boston)
NE: Pfiffner, Adrian O. [Hrsg.]

Cover photograph

The photo of the Swiss Alps in the Valais region displays (from left/east to right/west) the peaks of Monte Rosa, Breithorn, Matterhorn, Dent Blanche and Weisshorn.

The summit areas of Matterhorn, Dent Blanche and Weisshorn are erosional remnants of a large thrust sheet of crystalline basement derived from the Adriatic microplate, a spur of the African plate. This thrust sheet overlies a nappe complex that evolved from the subduction of the Piemont ocean and that extends from Breithorn to the lower slopes of Matterhorn, Dent Blanche and Weisshorn. Monte Rosa is carved out of crystalline basement pertaining to a still lower thrust sheet derived from the Briançonnais continental fragment. This entire nappe pile overlies the nappe stack derived from the Eurasian plate, which is buried deeply beneath the area of the photograph, as was imaged by seismic experiments of NRP 20.

Printed on acid-free paper produced from chlorine-free pulp TCF ∞
Printed in Switzerland
ISBN 3-7643-5254-X
ISBN 0-8176-5254-X

9 8 7 6 5 4 3 2 1

22 Integrated cross section and tectonic evolution of the Alps along the Eastern Traverse

S.M. Schmid, O.A. Pfiffner, G. Schönborn, N. Froitzheim and E. Kissling

Contents

22.1 Introduction

The Eastern Traverse follows closely the European GeoTraverse EGT (Figure 22-1, inset of Plate 22-1) and is partly based on geophysical data acquired in the framework of the EGT and earlier refraction seismic projects. These data are combined with data obtained during the NRP 20 project (Figure 22-1): line E1, almost parallel to the EGT line (see Pfiffner & Hitz, Chapter 9) and lines S1, S3 and S5 (see Schumacher, Chapter 10, projected into the Eastern Traverse, see also Holliger 1991). Whereas the Central and Western Traverses only offer relatively incomplete information across the entire Alps, both in respect to the geophysical methods used (only a few refraction lines are available) and in respect to their length (the Western Traverse stops well north of the Insubric line), the Eastern Traverse is nearly complete. Hence, to some extent and for certain authors (see Chapters 23 and 24) this section has model character. From a strictly geological point of view the position of the Eastern Traverse is ideal: it follows closely the N–S trending western margin of the Austroalpine nappes, which are largely missing further to the west and which almost completely cover lower structural units further to the east (Figure 22-1, inset of Plate 22-1). Proximity to this margin allows information on the Austroalpine units, projected into the profile. This enlarges considerably the cross section in a vertical direction. For example, in case of the southern Penninic units, downward extrapolation using geophysical data to depths of about 60 km can be complemented by an upward projection of geological units reaching 20 km above sea level. Furthermore, ongoing and very recent research outside the framework of NRP 20 offers further constraints on the geology along this transect: e.g. projects in the Bündnerschiefer (Steinmann 1994), the Adula nappe (Partzsch et al. 1994), the Austroalpine nappes and the Engadine line (Froitzheim et al. 1994, Schmid Froitzheim 1993), the Bergell area (Rosenberg et al. 1994 & 1995) and the Southern Alps (Schönborn 1992).

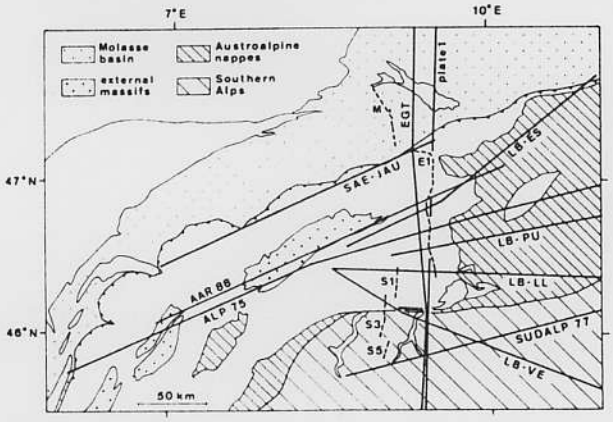

Figure 22-1
Network of seismic lines used for constraining the profile of plate 22-1. Solid lines: refraction profiles; broken lines: reflection profiles.

Plate 22-1 attempts to integrate geophysical and geological data into a single cross section across the Alpine chain. The section runs N–S along grid line 755 of the Swiss topographic map (except for the southernmost part near Milano, see Figure 22-1 and inset of Plate 22-1). As drawn, there is a marked difference between the tectonic style of the shallower crustal levels and that of the lower crustal levels. This difference in style is only partly real. The underlying wedging and associated deformation of the lower crust indeed strongly contrasts with the piling up and refolding of thin flakes of upper crustal material (the Alpine nappes), particularly in the central portion of the profile. This contrast is probably the most spectacular and unforeseen result of NRP 20.

Partly, however, this difference in style reflects the different types of data sets used for compiling this integrated cross section. Upper crustal levels have been drawn on the basis of projected surface information, locally constrained by the results of geophysical modelling (parts of the northern foreland and the Penninic nappes). The geometry of the lower crustal levels, on the other hand, relies entirely on the results of deep seismic soundings which provide a different scale of resolution compared to direct surface observation. It was felt that there was no point in drawing fine details into the deeper parts of the cross section, as is the case for the shallower parts, where such details are drawn according to projected surface information. As a result, lower and upper crustal levels may look more different in style and therefore less related than they probably are.

A word of caution concerns the use of this cross section. Deformation certainly was not plane strain within this N-S-section. Shortening, extension and displacements repeatedly occurred in and out of the section. For example, faults with a strike-slip component such as the Insubric line, currently juxtapose crustal segments whose internal structures may have developed elsewhere. Because this chapter is concerned primarily with a discussion of Plate 22-1, it will focus strongly on the cross-sectional view. However, the 3D problem will also be addressed. An appreciation of 3D problems in the Alps may be found in Laubscher (e.g. 1988,1991). For a discussion of 3D problems from a geophysical point of view the reader is referred to Pfiffner & Hitz (Chapter 9) and Valasek & Mueller (Chapter 23). An attempt to correlate different NRP 20 transects through the Alps from a geological point of view is found in Marchant & Stampfli (Chapter 24). Certain details of the Eastern Traverse interpretation in Chapter 24 differ from those given in this chapter.

22.2 Methods and data used for the compilation of the integrated cross section

The different parts of the cross section have been obtained by a variety of construction and projection methods. These methods, as well as the nature and quality of the geological and geophysical data, need to be outlined briefly for a better appreciation of the assumptions behind the methods and the nature of the data sources. After the discussion of the parts of the profile exhibiting the deep structure (compare also Valasek & Mueller, Chapter 23) the different parts of the higher structural levels will be discussed, proceeding from north to south.

22.2.1 Geophysical data used to compile features of the deep structure

The solid lines labelled "crustal model along EGT" denote the position of the upper and lower boundary of the lower crust, which is generally characterized by a significant increase in P-wave velocity and often high reflectivity

These lines are similar, but not identical to the C1/C2 (top of the lower crust) and M1/M2 (Moho) interfaces as defined in Chapters 9 and 23 and Valasek (1992). In Plate 22-1 the positions of these interfaces are drawn after the results of refraction work (Ye, 1992; Buness, 1992) and an integrated interpretation of both refraction and reflection seismic data (Holliger & Kissling 1992). This allows the reader to assess the degree of compatibility with the results obtained by the reflection method, also displayed in Plate 22-1. The positions of these interfaces depicted in Plate 22-1 do not differ significantly from those given by Valasek (1992). Positions where the interfaces are not well constrained are indicated by broken lines.
Only well-constrained seismic velocities from Ye (1992) are indicated in Plate 22-1 where they do not spatially overlap with the drawing of geological features. For clarity some of the fine details presented by Ye (1992) have been deleted. Velocities of around 6.5 to 6.6 km/s typical for the lower crust (with a notable exeption for the lower crust in the northern foreland according to Ye, 1992), contrast with values between 6.0 and 6.2 km/s in the lower parts of the upper crust. Layers characterized by lower velocities than those indicated in Plate 22-1, including velocity inversions, are observed at relatively shallow depth (Ye 1992). Low velocity layers (about 5.8 km/s) are found beneath the external Molasse basin at a depth of about 10km and also within the lower Penninic nappes and underneath the Southern Alps (see Ye 1992 for details).
The solid lines denoting the interfaces of the lower crust are constrained by migrated wide-angle reflections (modified after Hollinger & Kissling 1992 and Ye 1992). The position of these reflections is very strongly controlled by the availability of seven refraction profiles oriented parallel to the strike of the chain (Figure 22-1, see also Holliger & Kissling 1991, 1992, Baumann 1994). All these profiles intersect the profile of Plate 22-1 and the EGT refraction profile (Ye 1992), hence there is considerable 3D control on the position of these reflections. The depth migration procedure within the EGT profile (almost identical with the cross section of Plate 22-1) integrates new data by Ye (1992) and is outlined in Holliger (1991) and Holliger & Kissling (1991, 1992).

We chose to superimpose the results of reflection seismic work directly onto the features arrived at by refraction seismics in order to graphically visualize the degree of compatibility between these two data sets. Major deep reflections from the E1, S1, S3 and S5 lines (Figure 22-1) have been converted into digitized line drawings by a procedure outlined in Hollinger (1991). These digitized line drawings were projected onto the EGT line before migration in the N–S section. The eastward projection of data from the Southern Traverses was necessary in order to complete the profile along the Eastern Traverse, because E1 terminates well north of the Insubric line. The chosen procedure for eastward projection needs to be briefly discussed.
Any projection method assumes lateral continuity of the structures projected. However, if structures from different tectonic levels do depart from each other in terms of direction and plunge of the projection vector, the question will then arise, which structure one assumes to be laterally continuous. Marchant (1993) and Marchant & Stampfli (Chapter 24) put the large dimensions of the Adriatic lower crustal wedge below the Penninic nappes (at a depth of 20 to 50km in the center of Plate 22-1) into question by arguing that the N-wards flattening Insubric line, well imaged along S1, has to be projected to the east by using the axial dip of the Adula nappe. By cylindrically projecting the Adula and underlying Penninic nappes, including the Insubric line above the Adriatic lower crustal wedge, to the E, there is of course no room for such a large wedge. This is because the S-dipping lower crust of the northern foreland does not exhibit such an axial dip to the E. Conversely, if one projects those parts of the lower crustal wedge covered by S1, including the Insubric line, subhorizontally to the east (Hollinger 1991) there is no room for Penninic units below the Leventina-Lucomagno nappe along the Eastern Traverse, as depicted in Plate 22-1.

Holliger (1991) and Holliger & Kissling (1991, 1992) have argued that the geometry of middle to lower crustal material is appropriately constrained by Bouguer gravity data (corrected for the effects of the Ivrea body, Kissling 1980, 1982). This gravity map reflects the integrated effects of such deep crustal features. This then ultimately (i.e. after migration) leads to the configuration depicted in Plate 22-1. The following major arguments additionally support the procedure chosen: (1) There is independent evidence for the existence of such a large lower crustal wedge from the refraction work carried out along the EGT line (Ye 1992) and the compatibility of the refraction-based model of Ye (1992) with the projected and migrated line drawings of the major reflections is good as can be seen in Plate 22-1. (2) The axial dip of the Alpine nappes to the east is discordant to the European lower crust and the Moho, independently indicating strong decoupling between lower and upper crust. In the light of this decoupling the use of a cylindrical projection of upper crustal flakes is, in our view, not justified for projecting lower crustal features such as the Adriatic wedge.

In a second step, the projected digitized line drawings were migrated according to a velocity model which needs no projection since it is based on strike-parallel profiles (Holliger 1991). This velocity model (figure 4 in Holliger and Kissling 1992) is the same as that used for the migration of the wide-angle reflections discussed earlier. The picture emerging from this procedure shows excellent consistency between refraction and reflection data and one geological feature which can be traced to great depth: the Insubric line.

Except for a reflectivity gap beneath the internal Aar massif and the Gotthard "massif" there is excellent agreement between the position of the lower crust of the northern foreland derived from refraction work (solid lines in Plate 22-1) and the zone of high reflectivity. The reason for this gap in near-vertical reflections is not completely understood but it is unlikely to represent a gap in the European Moho as postulated by Laubscher (1994). On the contrary, wide-angle data from the EGT profile and from several orogen-parallel profiles (Figure 22-1) show strong seismic phases from the Moho in this region (Kissling 1993; Ye et al. 1995), whose position is indicated by a solid line in Figure 22-2a (Holliger and Kissling 1991). By applying a NMO (normal-move-out) correction, Valasek et al. (1991) displayed these wide-angle Moho reflections along the EGT profile in a manner commonly used for near-vertical reflection data (Figure 22-2b). Hence, Figure 22-2 clearly documents the continuity of the Moho beneath the northern foreland and the entire Penninic realm.
The gap in the lower crustal reflections in the near-vertical reflection profile is at least partly due to the projection and migration procedures: The northern termination of the southern portion of high reflectivity coincides with the northern termination of profile S1 and is thus a projection artefact. The southward termination of the northern part of reflective lower crust is most likely caused by imaging problems (Holliger 1991, Valasek 1992).
The reflections from the lower crustal Adriatic wedge cross each other in many places, indicating discontinuities within the wedge or, alternatively, problems with the projection and/or migration procedures. As pointed out by Holliger & Kissling (1992) the lower crustal wedge may have a complicated internal structure representing a mixture of predominantly Adriatic lower crust and oceanic crust, having a density slightly higher than that of "normal" lower crust. It is clear, however, that this zone of high reflectivity is largely contained within the lower crustal wedge of the refraction-based EGT crustal model (solid lines in Plate 22-1) except for some gently N-dipping reflections at a depth of 20–25km, slightly above the upper boundary of the lower crustal wedge according to refraction work (solid line below grid 140 in Plate 22-1).
Prominent steeply inclined reflections recorded along line S1 commonly related to the Insubric line (Bernoulli et al. 1990, Holliger 1991, Holliger and Kissling 1991, 1992) project into a surface location 5–10km north of the Insubric line in Plate 22-1 (within the northern part of the southern steep belt, near the axial trace of the Cressim antiform). However, due to inaccuracies in the projection and migration techniques, the exact location of some of these reflections in relation to the Insubric mylonite belt remains speculative. In view of the parallelism between the Insubric mylonite belt and the southern steep zone (Schmid et al. 1989) these reflections can be taken to document a flattening of the Insubric mylonite belt from the 70° inclination measured at the surface (Schmid et al. 1987, 1989) to about 45° at some 20km depth.

22.2.2 Helvetic nappes and northern foreland

The top of basement is only accessible to surface observation in the Vättis window (Aar massif) along the profile of Plate 22-1. The geometry chosen for the structure of the top of basement is that of model 1, discussed in Stäuble & Pfiffner (1991 b) and Pfiffner et al. (Chapter 13.1). These authors compared the seismic responses of four alternative geometries (models 1-4) generated by 2D normal-incidence and offset ray tracing with the reflection seismic data. They produced the best-matching events with this particular model 1. Thrusts and folds in the Subalpine Molasse are constructed on the basis of surface data and projected information obtained from a reflection seismic profile, recorded for hydrocarbon exploration, situated immediately west of the EGT traverse (profile M in Figure 22-1; Stäuble & Pfiffner 1991a and Pfiffner et al., Chapter 8).
The Helvetic nappes are only partly constructed according to extrapolation of surface information obtained along the profile trace. Certain details are drawn according to the results of 3D modelling of reflection seismic data (Stäuble et al. 1993). The higher Penninic and Austroalpine units overlying the Helvetic nappes are only exposed east of the transect and have been projected onto the profile parallel to a N 70° E azimuth by using profiles published by Allemann & Schwizer (1979) and Nänny (1948). Updoming of the base of the Austroalpine nappes above the Aar massif corresponds to the Prättigau half window in map view (Cadisch 1950; see also Pfiffner & Hitz, Chapter 9). Its geometry was obtained by stacking a series of profiles across the Prättigau half window (Nänny 1948). Stacking did not use a fixed axial plunge, but instead resulted from lateral correlation between individual pro-

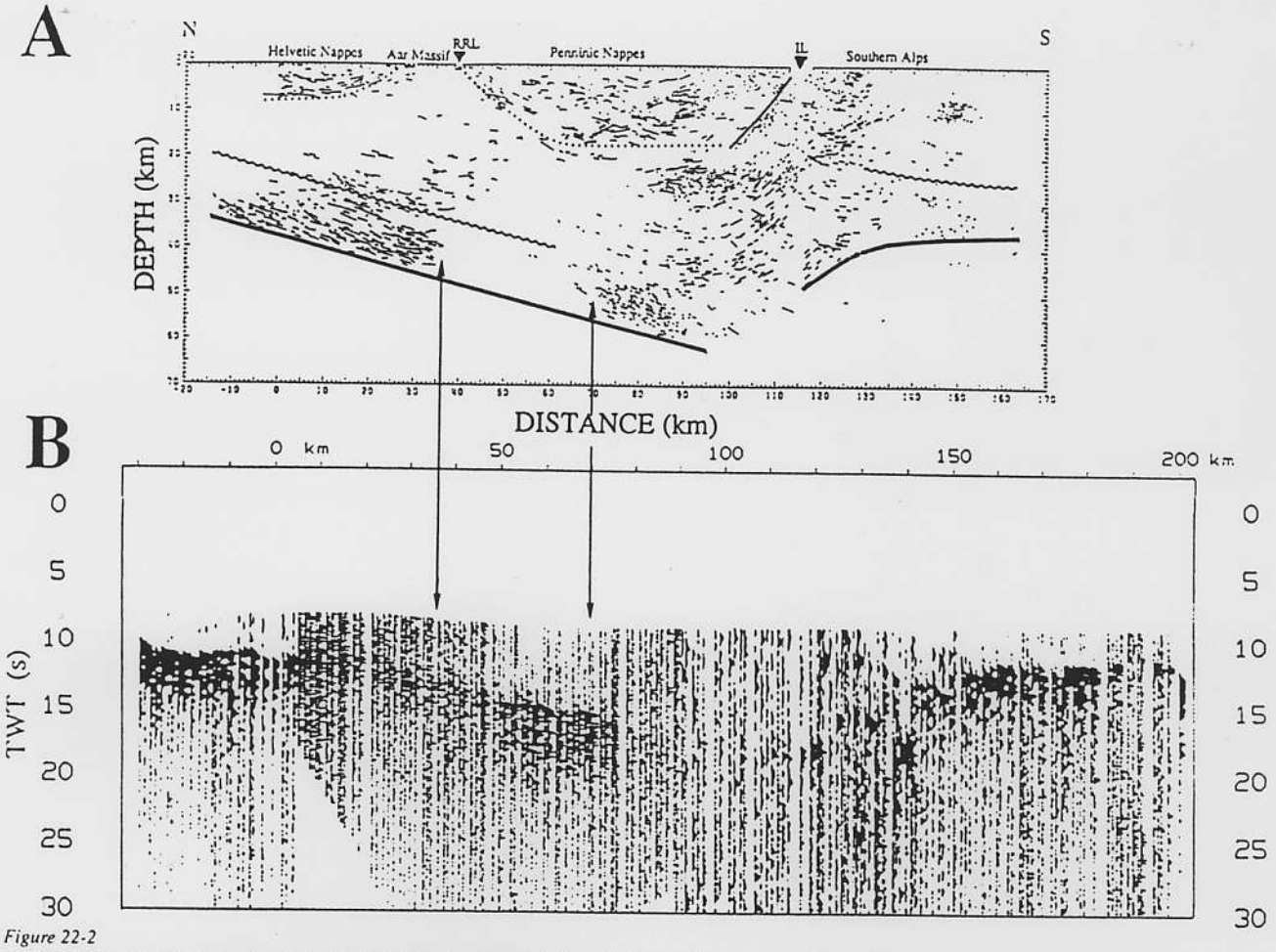

Figure 22-2

Summary of seismically determined crustal structure and Moho depth along the Eastern Traverse (see plate 22-1).

a: Migrated near-vertical reflections along the Eastern Traverse and generalized seismic crustal structure derived from orogen-parallel refraction profiles (Hollinger & Kissling 1992). Solid line: position of Moho, derived from orogen-parallel refraction profiles; wiggly line: top lower crust; dotted line: base of Penninic and Helvetic nappes; thin solid line: Insubric Line (IL); RRL: Rhine-Rhone Line.

b: Normal incidence representation of the wide-angle Moho-reflections in the EGT refraction profile perpendicular to the orogen and across the eastern Swiss Alps (Valasek et al. 1991).

files. The geometry thus obtained (Plate 22-1) results in an average plunge of 15° for the culmination of the base of the Austroalpine units, as can be determined from the vertical and horizontal distances between a point situated in the Vättis window and the eastern termination of the Prättigau half window near Klosters. This angle agrees closely with the plunge of the axial culmination of the Aar massif, based on the network of the seismic profiles E1, E7, E8, E9 and E10 (Hitz & Pfiffner 1994 and Chapter 9).

22.2.3 The Gotthard "massif" and the transition into the lower Penninic nappes

Very strong reflections dipping southward from 2.5 to 4.0 s TWT along line E1 between Canova and Thusis (reflector D in plate 4 of Pfiffner et al., 1990b) have been interpreted in Plate 22-1 (between grid lines 175 and 190) to be due to the allochthonous cover of the southern Gotthard "massif" (Etter 1987). The existence of the small Tavetsch massif as far east as our transect is considered unlikely, as discussed in more detail in Chapter 9. However, an alternative interpretation, such as model A of Pfiffner et al. (1990 b), which attributes this band of S-dipping strong reflections to the top of the Aar massif, cannot be ruled out. According to this alternative model the Gotthard "massif" would wedge out west of the transect discussed here (but see Chapter 9).

The Penninic basal thrust is placed immediately above the inferred allochthonous cover of the Gotthard "massif" (labelled "Triassic, Lower and Middle Jurassic cover slices" in Plate 22-1) according to the final 3D model of the Penninic units given by Litak et al. (1993). Earlier interpretations based on N-dipping reflections visible under the Gotthard massif (northern termination of reflection group E in plate 4 of Pfiffner et al. 1990b), advocating backthrusting and/or backfolding of the Gotthard massif (model C in Pfiffner et al. 1990 b) are abandoned. Seismic modelling showed that these N-dipping reflections may be caused by a synform situated at the base of the Adula nappe near the northern termination of the Simano nappe (see Plate 22-1).

According to the geological interpretation given in Plate 22-1, the basal thrust of the Gotthard "massiv", the Urseren-Garvera zone, is steeply inclined and is therefore not imaged seismically. Regardless of the uncertainties in interpreting the exact shapes of the southernmost Aar massif and the Gotthard "massif", and based on the geometry constrained by 3D seismic modelling (Figure 3a in Litak et al. 1993), the Penninic basal thrust is not shown to be strongly backfolded but merely steepened up in Plate 22-1. This is important since it marks a substantial change in structural style from the Lukmanier area (Etter 1987, Probst 1980). In the Lukmanier area, a late deformation phase (Figure 22-3) linked to the formation of the Chiera synform (D3 of Etter 1987) and to the Carassino phase in the frontal Adula nappe (Löw 1987) leads to substantial backfolding. Such backfolding is even more pronounced in the southern part of the external massifs of the Western Traverse (see Alpine cross section by Escher et al. presented in Chapter 16). This severe overprint by backfolding apparently dies out eastward.

The Gotthard "massif" is considered as a lowermost Penninic, or more exactly a "Subpenninic" nappe (Milnes 1974), in a structural sense. These Subpenninic units also include the Lucomagno-Leventina and Simano nappes, whose geometry will be discussed later. There is a serious problem with the use of terms like "Helvetic" and "Penninic" in that, for historical reasons, they may refer to paleogeographic domains and/or structural units. Whereas the Lucomagno-Leventina and Simano nappes, and according to our interpretation also the Gotthard "massif", may be described as Penninic in a structural sense, it is very likely that some of this crystalline basement represents basement to the Helvetic and Ultrahelvetic cover nappes. This is supported directly by the facies of the overturned allochthonous cover of the southern Gotthard "massif" (Etter 1987, Jung 1963, Frey 1967) which has close affinities with the Helvetic sediments. Use of he term "Subpenninic" helps to resolve this dilemma.

To the west, Trümpy (1969) considers the Tavetsch massif to represent the substratum of the Helvetic nappes in general, whereas Pfiffner (1985) and Wyss (1986) only attribute the Axen nappe to this massif and the Säntis-Drusberg nappe to the Gotthard "massif". Within the transect of Plate 22-1, the structural separation amongst individual Helvetic nappes above the Glarus thrust diminishes in importance. In the profile considered here, the Säntis thrust separates the Jurassic strata of the Lower Glarus nappe complex from the Cretaceous strata of the Upper Glarus nappe complex (Pfiffner 1981). The Säntis thrust has acted primarily as a structural discontinuity separating different styles of shortening within the Jurassic and Cretaceous strata. Displacement across the Säntis thrust decreases steadily southward and eastward due to imbrications in the Jurassic strata (Stäuble et al. 1993). Bed length measured in the Upper Jurassic limestone (38 km) is very similar to that measured in the Cretaceous Schrattenkalk (33 km, see Plate 22-1). Hence, both stratigraphic levels must be assigned to the same basement, contrary to findings further west, where the Axen nappe incorporates both Jurassic and Cretaceous strata while the Säntis-Drusberg nappe consists of Cretaceous sediments only, Jurassic strata having been left behind.

This leads to the question as to wether the entire Glarus nappe complex is rooted in the Tavetsch massif (Trümpy 1969), or alternatively, within the Subpenninic nappes. We prefer the second option in view of the considerable difficulties of finding appropriate volumes of upper crustal basement material within the Tavetsch massif. In map view, the Tavetsch massif pinches out eastward and is unlikely to be encountered beneath the transect of line E1. The excess volume of upper crust provided by the updoming of the Aar massif is ruled out from the search for appropriate basement material. This excess volume is caused by some 27 km of crustal shortening post-dating the detachment of the Helvetic nappes and related to imbrications in the Subalpine Molasse (Burkhard 1990, Pfiffner 1986, Pfiffner et al. 1990b). In order to accommodate the 38 km bed-length of Helvetic nappes (assuming plane strain conditions and an upper crustal thickness of 15 km) an area of about 570 km^2 of upper crustal material has to be identified somewhere in Plate 22-1. This suggests that both the Gotthard "massif" and the Lucomagno-Leventina nappe (occupying about 540 km^2 in our section) may represent this upper crustal basement of the Helvetic nappes, their original cover having been substituted by sediments of a more southerly provenance during early phases of detachment.

22.2.4 The northern and central parts of the Penninic zone

Most of the surface data used for constructing this part of the profile (Plate 22-1) have been presented in Chapter 14. This information has been supplemented by data from Steinmann (1994) covering the area of the North-Penninic Bündnerschiefer. Details concerning the orogenic lid (the Austroalpine units) have been improved in respect to an earlier version of parts of this profile (figure 2 in Schmid et al. 1990) using new data from Froitzheim et al. (1994), Handy et al. (1993), and Liniger (1992).

In a first step all major tectonic boundaries have been projected strictly parallel to a N 70° E direction up and down plunge. This direction approximates best the azimuth of most large-scale fold structures in this region. A series of sections parallel to N 70° E, constructed on the basis of structure contour maps, allowed for projections with variable plunge (10-35°). Units were projected into the profile along these strike-parallel sections by assuming that their thicknesses do not change along strike. Geological details within projected units are drawn according to the geometries found where these units are exposed.

In a second step this part of the profile was adjusted to conform to the 3D model based on seismic information (Litak et al. 1993 and Pfiffner & Hitz, Chapter 9). These adjustments were relatively minor at shallower depths and above the Adula nappe. The most important modification concerns the Misox zone, which has a considerable thickness and which is shown to be continuous southward, joining up with the Chiavenna ophiolites exposed at the surface. This is in contrast to surface geology exposed west of the profile, where the Misox zone is cut out near the Forcola pass due to top-to-the-east movements along the Forcola normal fault. The Chiavenna ophiolite is portrayed as a long continuous slab, about 1 km thick, which caused high-amplitude reflections consistent with a gneiss/ophiolite interface (Litak et al. 1993).

The overall geometry of the Adula and Simano nappes follows that given in figure 3a of Litak et al. (1993). Ornamentation in the Adula nappe is based on the data of Löw (1987). A considerable amount of speculation led to the depicted geometry of the top of the Gotthard "massif" and the Lucomagno-Leventina units. While their overall position below the Penninic basal thrust is constrained by the model of Litak et al. (1993), the portrayed structural details are based on surface information a long way west of the transect. This information, which was taken from profiles by Etter (1987), Löw (1987), and Probst (1980), had to be modified significantly in order to conform to constraints imposed by the geometry of the Penninic basal thrust. Major synformal zones such as the Scopi, Piora, and Molare structures appear more flat-lying in Plate 22-1 than they are further to the west, since they are interpreted to be unaffected by the Chiera synform as discussed earlier.

As seen from Plate 22-1, there is no room for additional Subpenninic thrust sheets between the Lucomagno-Leventina nappe and the Adriatic lower crustal wedge. This is a corollary of combining refraction data (top Adriatic wedge) and reflection data (position of the top of the Leventina-Lucomagno nappe). Such lower units do exist beneath the S3 line (Bernoulli et al. 1990), but they are interpreted to wedge out eastward.

22.2.5 Southern Penninic zone, Bergell pluton and Insubric line

In the area of the Bergell (Bregaglia) pluton (Trommsdorff & Nievergelt 1983) the geological profile is based on recent work by Rosenberg et al. (1994 & 1995) and Davidson et al. (in press). Some new findings, particularly relevant to the methods of profile construction and the discussion of the tectonic evolution along this transect, need to be outlined briefly.

In its northern part, the Bergell pluton tectonically overlies the upper amphibolite to granulite grade migmatitic rocks of the so-called Gruf complex (Bucher-Nurminen & Droop 1983, Droop & Bucher-Nurminen 1984). Structural work in progress unambiguously demonstrates that the Gruf complex continues into the migmatites forming the southernmost part of the Adula nappe (Hafner 1994). These migmatites have been backfolded around the Cressim antiform (Plate 22-1, Heitzmann 1975). Therefore the Gruf complex, including the window below the Bergell pluton at Bagni di Masino, has to be considered part of the Adula nappe.

Whereas quartzo-feldspatic gneisses predominate within the Gruf complex, a variety of other lithologies consisting of ultramafics, amphibolites, calc-silicates and alumo-silicates is concentrated in an almost continuous band concordantly following the tonalitic base of the Bergell pluton. The base of this intrusion is exposed along its western margin and in the Bagni di Masino window (Wenk & Cornelius 1977, Diethelm 1989). Near Vicosoprano a narrow antiform within the Gruf complex immediately south of the Engadine line (indicated in Plate 22-1 according to work in progress) is interpreted to connect these lithologies at the base of the pluton with the Chiavenna ophiolites. The Chiavenna ophiolites overlie the Gruf complex along a steeply north-dipping faulted contact (Schmutz 1976), which is possibly related to movements along the Engadine line. Hence, this band of ultramafics and metasediments found on top of the Gruf complex is tentatively interpreted to be the southern continuation of the Chiavenna ophiolites and the Misox zone.

Based on this interpretation, and independent of the correlation between the Adula nappe and Gruf complex, the Bergell pluton appears to occupy a similar structural position to that of the Tambo and Suretta nappes north of the Engadine line. Recent mapping near Vicosoprano has revealed the following geometry shown in Plate 22-1, which supports this conclusion: The granodiorite cuts discordantly through the remnants of both theTambo and Suretta nappes that are preserved south of the Engadine line. Over the short distance between Vicosoprano and the Maloja pass the northern contact of the Bergell pluton reaches higher tectonic levels exposed along its eastern margin (i.e. Avers Bündnerschiefer and Forno-Lizun ophiolites).

Magmatic, submagmatic and solid state deformational fabrics in tonalite, granodiorite, and country rocks show that the Bergell pluton was emplaced and solidified during a regional tectonic event. This synmagmatic deformation first produced a very strong (mylonitic) fabric found at the base of the pluton and, subsequently, led to large-scale folds that shortened this basal contact (Plate 22-1). One of these folds can be traced directly into the Cressim antiform (Hafner 1994, Plate1).

Initial stages of vertical movement along the Insubric mylonite belt affected the tonalitic tail of the southern Bergell pluton and were coeval with deformation in the presence of melts (Rosenberg et al. 1995). This conclusion is contrary to earlier interpretations, which regarded all movements along the Insubric line to postdate the Bergell intrusion (Schmid et al. 1987). It also shows that final intrusion, backfolding and initial stages of backthrusting along the Insubric line were contemporaneous and related to ongoing N–S shortening. The north-dipping Insubric mylonite belt was extrapolated to depth by assuming that it parallels the migrated reflections attributed to the Southern Steep Belt (Plate 22-1). The vertical, brittle Tonale fault (as exposed in a spectacular gorge near Gravedona, Fumasoli 1974) is related to later strike-slip movements along the Insubric line.

Considerable vertical extrapolation is possible thanks to the pronounced ax-

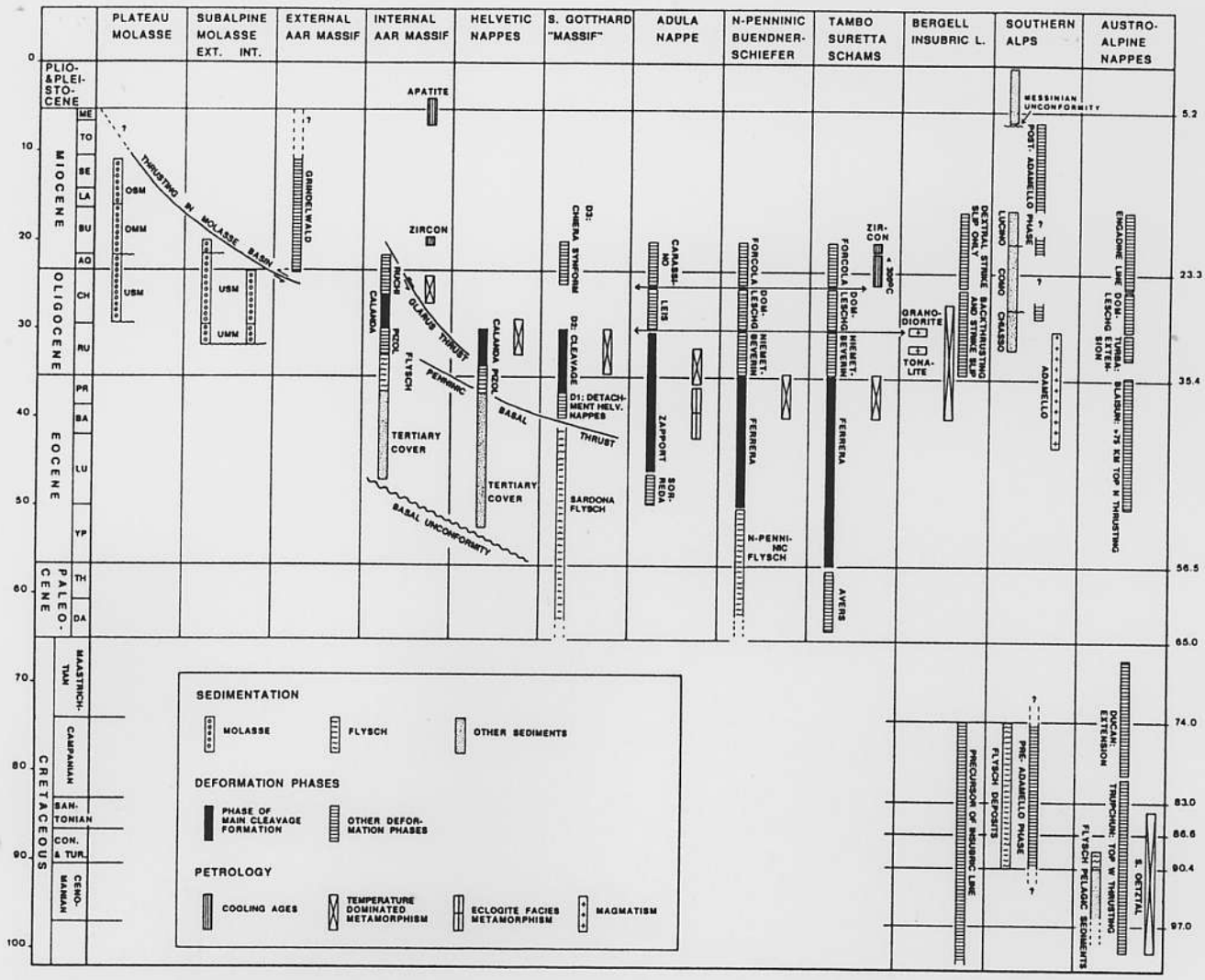

Figure 22-3
Correlation table, showing an attempt to date deformation phases and metamorphism along the Eastern Traverse. Time scale according to Harland et al. (1989). See text for further explanations. For details concerning the Penninic units compare with Chapter 14.

ial plunge of the Bergell pluton indicated by structural (Rosenberg et al. 1994 & 1995) and petrological (Reusser 1987) data. In a first step, the Tambo and Suretta nappes were projected southward and upward by using structure contour maps (Pfiffner et al. 1990a, partly modified by new field data). At a point situated near Vicosoprano, east of the transect (projecting well above sea level in Plate 22-1) the geometries of Tambo, Suretta and overlying nappes were displaced vertically across the Engadine line by 4 km, in accordance with the kinematic model for this line proposed by Schmid and Froitzheim (1993). Using this kinematic model, the position of the Tambo and structurally higher tectonic units was anchored to their position immediately south of the Engadine line where these nappes were cut by the Bergell intrusion.

The position of the base of the Bergell intrusion was evaluated by projecting auxiliary profiles located east of Plate 22-1. This projection used structure contour maps (Davidson et al., in press) of the base of the pluton, deformed by NE–SW striking folds. The roof of the intrusion was placed at the structural level presently exposed at the eastern margin of the pluton. This is a minimum altitude, since the eastern contact represents the side rather than the roof of this pluton (Rosenberg et al. 1995, Spillmann 1993). The geometry of the "Ultrapenninic" (in the sense of Trümpy 1992) or Austroalpine Margna and Sella nappes, including the continuation of the southward outwedging Platta ophiolites and the Corvatsch-Bernina nappes, is drawn after Liniger (1992) and Spillmann (1993). However, this geometry is exposed approximately 25 km east of the transect and may be substantially different in our transect. This geometry was projected nevertheless in order to illustrate the southward connection of the orogenic lid to the Austroalpine Tonale series exposed in the Southern Steep Belt north of the Insubric line.

22.2.6 Southern Alps

The Southern Alps part of the section was taken without modification from Schönborn (1992, cross section B of his enclosure) except for the northernmost region where compatibility with the shape of the Insubric fault necessitated very minor adjustments. This section in Schönborn (1992) almost coincides with N–S grid line 755, departing from a N–S orientation only south of E–W grid line 60 in order to incorporate well data published by Pieri & Groppi (1981).

The profile is balanced and retro-deformability was established at all stages by forward modelling. The deeper parts of the profile were kept as simple as possible and drawn according to geometrical rules of ramp and flat geometry observed for basement and cover the surface. More intensive dissection by thrusting and/or ductile lobes, comparable to those proposed for the Aar massif, is to be expected, but has not been drawn because of the lack of subsurface data. However, the mass balance within the basement, the top of which is well constrained by well data in its undeformed portion in front of the Milan thrust belt (Plate 22-1) is unaffected by geometrical details. The total amount of shortening (about 80km) within the sediments necessarily leads to the postulate that parts of the upper crustal and all of the lower crustal excess volume must now occur within the Adriatic wedge situated below the Penninic nappes and the depth extrapolation of the N-dipping Insubric line. The volume of crustal material available south of the Insubric line is insufficient (Schönborn 1992, Pfiffner 1992). Substantial thinning of the Adriatic lower crust during Jurassic rifting and passive continental margin formation cannot be held responsible for this volume deficit because the Southern Alps were in a lower plate margin situation at that time (Lemoine et al. 1987, Froitzheim and Eberli 1990).

In order to allow for a change in structural style within the deeper basement, ductile shear zones have been schematically drawn at depth. These shear zones are expected to merge with a major detachment zone situated at the interface between the upper and lower Adriatic crust. This major detachment allows for the northward indentation of the Adriatic lower crust, or conversely, for southward transport of the Insubric line, together with the Central Alps, over the Adriatic lower crust.

22.3 Summary of the tectonic evolution

The tectonic evolution of the Alps along the Eastern Traverse (the Penninic units are discussed more extensively by Schmid et al. in Chapter 14) will be summarized with the help of the profiles presented in Figure 22-7 (identical to Figure 14-21). The timetable of Figure 22-3 (identical to Figure 14-20) provides the available time constraints.

22.3.1 Paleotectonic reconstruction

Three former oceanic basins controlled the paleogeography of the Alps: the Hallstatt-Meliata, the Piemont-Liguria and the Valais oceans (Figure 22-4). While remnants of the Piemont-Liguria and Valais oceans are found in the form of ophiolitic slivers along the cross section discussed here (compare discussion in Chapter 14), remnants of the Hallstatt-Meliata ocean are only found further to the east (Eastern Alps of Austria, Carpathians). However, because this ocean played an important role during Cretaceous orogeny, it needs to be discussed briefly here.

The Hallstatt-Meliata ocean opened during the Middle Triassic in a position southeast of the present Austroalpine realm (Kozur 1992) and it may have been connected to the Vardar ocean of the Dinarides and Hellenides. Its paleogeographic position is indicated in the sketch of Figure 22-4. Triassic sediments of the Austroalpine units record the history of the shelf and passive margin of Apulia that faced this ocean (Lein 1987). The Mid-Triassic rifting that led to the opening of this ocean is spatially unrelated to the Late Triassic to Early Jurassic rifting leading to the opening of the Piemont-Liguria ocean which will form at the northwestern margin of the Apulian microcontinent (western part of the Austroalpine nappes, Southern Alps). The remnants of this ocean did not reach the region of the profile of Plate 22-1. However, Cretaceous or "Eoalpine" orogeny resulting from continental collision following the closure of the Hallstatt-Meliata ocean during the Early Cretaceous also affected the Austroalpine and South-Penninic units in our transect. This collision was followed by westward propagation of a thrust wedge towards our area of interest in eastern Switzerland (Thöni and Jagoutz 1993, Neubauer 1994).

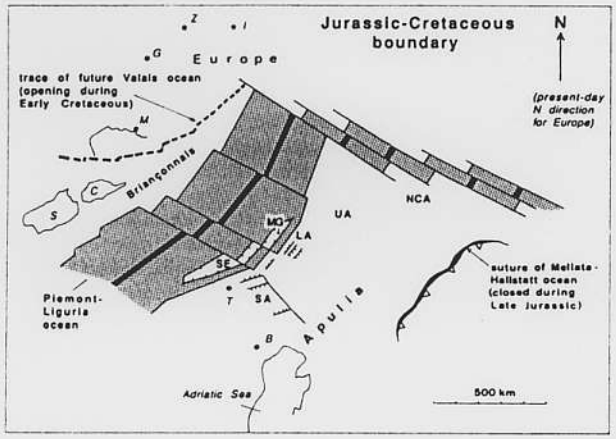

Figure 22-4
Paleogeographic reconstruction of the Piemont-Liguria (South Penninic) and the Hallstatt-Meliata ocean and their margins at the Jurassic-Cretaceous boundary, after Dercourt et al. (1986) and Stampfli (1993). SE: Sesia-Dentblanche extensional allochthon; MG: Margna extensional allochthon; SA: passive continental margin of Southern Alps; LA: Lower Austroalpine realm; UA: Upper Austroalpine realm; NCA: Northern Calcareous Alps. Geographical reference points are: S (Sardinia), C (Corsica), M (Marseille), G (Geneva), Z (Zürich), I (Innsbruck), T (Torino) and B (Bologna).

The passive continental margin along the northwestern edge of the Apulian microcontinent is locally well preserved in spite of crustal shortening in the Austroalpine nappes of eastern Switzerland (Froitzheim & Eberli 1990, Conti et al. 1994) and in the Southern Alps (Bertotti 1991, Bertotti et al. 1993, Schumacher et al., Chapter 15). During the final rifting phase (Toarcian to Middle Jurassic) a system of west-dipping detachments formed, probably penetrating the whole lithosphere and accommodating simple-shear extension (Froitzheim & Manatschal in press). The passive margin preserved in the Austroalpine nappes of Graubünden (Figure 22-5) is amazingly similar to that preserved in the Southern Alps (Bernoulli et al. 1993); both areas exhibit features typical for a lower plate margin.

The present Margna-Sella nappe system occupied a special position near the passive continental margin at the northwestern edge of the Apulian microcontinent. Following Trümpy (1992) we have separated these "Ultrapenninic" units from the lower Austroalpine nappes with the Corvatsch-Bernina units at their base in the profile of Plate 22-1. According to Froitzheim & Manatschal (in press) the Margna-Sella nappes in Graubünden and the Dent Blanche-Sesia units of the Western Alps represent extensional allochthons that became separated from the Apulian margin by a narrow intervening zone of denudated mantle rocks (Platta unit in Plate 22-1) before the formation of a mid-oceanic ridge west of these extensional allochthons (Figures 22-4 and 22-5). The present structural position of the Margna-Sella nappes below the Platta ophiolites and above the Forno-Malenco ophiolites (Figure 22-6b) reflects the influence of complications in the paleogeography according to Liniger (1992) and Spillmann (1993). According to the reconstruction depicted in Figure 22-5 there is no need for the former existence of an additional spreading centre south of the Margna-Sella extensional allochthon.

An upper plate position of the Briançonnais unit in respect to the Piemont-Liguria ocean is inferred by most authors. However, the geometry of the margin facing the Valais ocean, which probably did not open before the Late Jurassic to Early Cretaceous (Frisch 1979, Florineth & Froitzheim 1994, Stampfli 1993, Steinmann 1994), is ill-constrained. The reconstruction depicted in Figure 22-7a shows an upper-plate position of the Briançonnais with respect to the Valais ocean in order to minimize the volume of continental crust underlying the Briançonnais facies domain (compare Figure 14-8 in Chapter 14). Note, however, that Florineth & Froitzheim (1994) present local field evidence in favour of a lower-plate margin at the NW edge of the Briançonnais. Evidence for sinistral strike slip motion between Europe and the Briançonnais terrane (Stampfli 1993) and for local sinistral transpression in the Schams nappes (discussion in Chapter 14, Rück 1990, 1995, Schmid et al 1990) points to very oblique opening, not necessarily leading to a single predominating asymmetry.

The proposed paleogeographic situation of the Adula nappe at the distal margin of stable Europe (Figure 22-7a; see also Schmid et al. 1990, and Chapter 14) has far-reaching consequences regarding the timing of eclogite facies metamorphism in the Adula nappe (a Tertiary rather than Cretaceous age is the corollary), the width of the European distal margin that has been subducted (more than usually assumed and in accordance with the estimates of Marchant & Stampfli, Chapter 23), and the very high rates of subduction and subsequent exhumation of the Adula eclogites. In order to minimize the amount and rate of Tertiary subduction, a width of only 50km was assumed for that part of the Valais or North-Penninic Bündnerschiefer basin that was originally underlain by oceanic crust (Figure 22-7a).

22.3.2 Cretaceous (Eoalpine) orogeny

Figures 22-5 and 22-6 illustrate that the Austroalpine nappe pile in eastern Switzerland was assembled by oblique east-over-west imbrication of the NW passive margin of the Apulian microcontinent (Froitzheim et al. 1994, Handy et al. 1993, Schmid & Haas 1989). The associated deformation (Trupchun phase in Figure 22-3; see Froitzheim et al. 1994) also affected structurally lower units, such as the Arosa-Platta ophiolites, the "Ultrapenninic" Margna-Sella nappes and the Lizun-Forno-Malenco ophiolites underlying the Margna nappe (Ring et al. 1988, Liniger 1992, Spillmann 1993). During Tertiary orogeny a basal thrust displaced all these structurally highest units that were previously affected by Cretaceous orogeny to the north by at least 75km (Froitzheim et al. 1994). This orogenic lid in the sense of Laubscher (1983) overrode the present day Engadine window and the Prättigau half-window (between coordinates 190 and 210 in the profile of Plate 22-1) only after Cretaceous orogeny. Sedimentation in the Briançonnais and Valais domains through to the Early Tertiary precludes Cretaceous orogeny within these lower structural units.

We propose separate orogenies during the Cretaceous and Tertiary, rather than two separate deformation phases during progressive convergence for the following reasons:

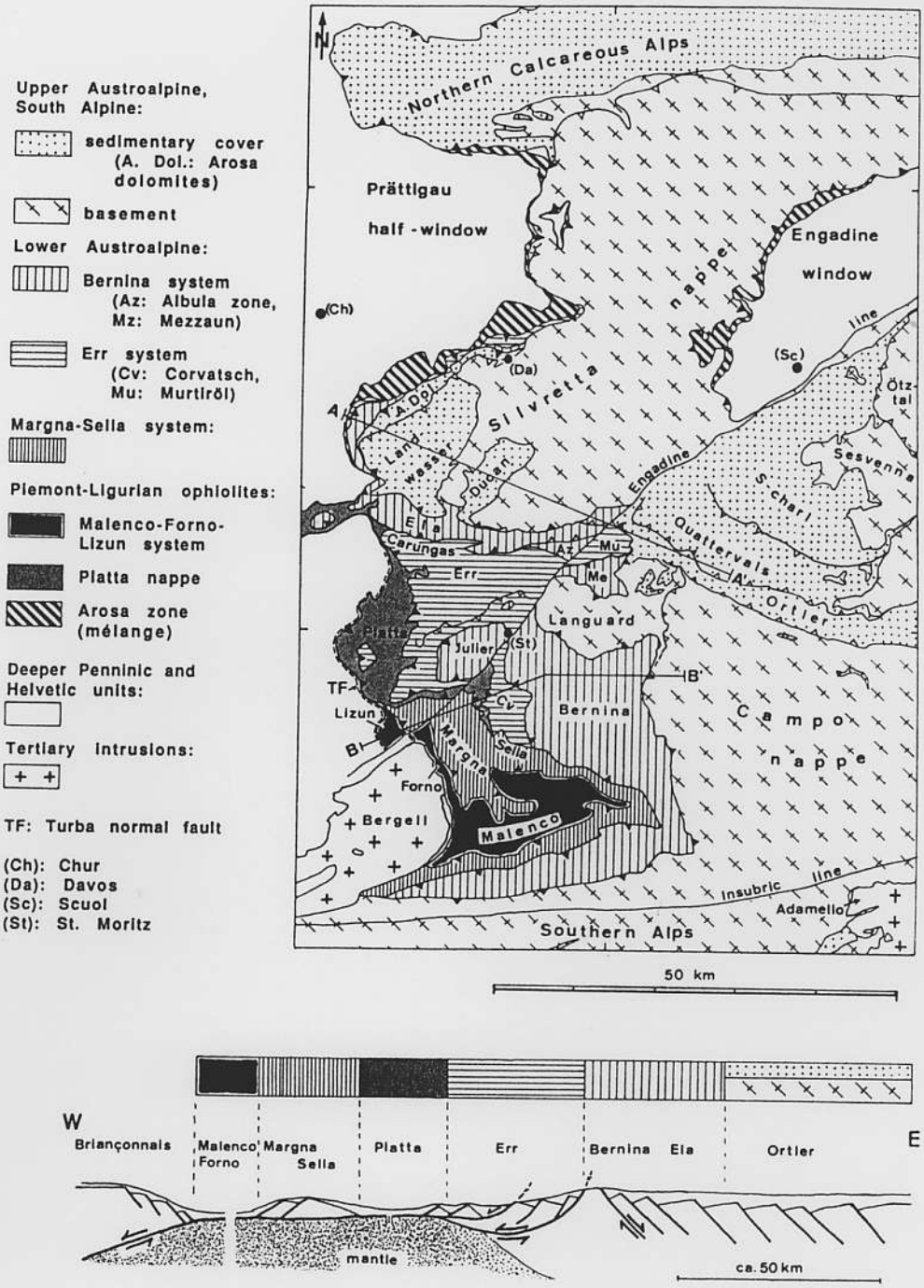

Figure 22-5
Reconstructed E–W section through the passive margin preserved in the Austroalpine units of Graubünden (bottom figure from Froitzheim et al. 1994) and map of the tectonic units in the Austroalpine realm, representing westwardly dislocated fragments of this passive continental margin. Small triangles along tectonic boundaries point in the direction of the structurally higher unit, irrespective of the nature of the boundary (thrust or normal fault; for details see Froitzheim et al. 1994).

(1) The kinematics (top to the W–WNW imbrication associated with orogen-parallel strike slip movements) of the Cretaceous orogeny are totally different from the top to the N–NNW movements characteristic of the Tertiary orogeny.
(2) A Late Cretaceous period of extensional collapse, to be discussed below, provides a clear temporal hiatus between the two orogenies.
(3) Subduction associated with eclogite facies metamorphism took place twice in the Alps: first during the Cretaceous and then during the Tertiary. Cretaceous-aged subduction occurred before the closing of the Piemont-Liguria ocean, encompassing subduction of continental slices within the Austroalpine domain (collision due to the closing of the Hallstatt-Meliata ocean, eclogites within the Austroalpine units of Austria) and subduction of extensional allochthons situated near the active northwestern margin of Apulia (eclogites in the Sesia zone). Tertiary-aged subduction of European and Briançonnais continental crust (e.g. in the Adula nappe) is related to the closing of the Valais and Piemont-Liguria oceans as a consequence of collisions during Tertiary orogeny.

Nappe imbrication during the Trupchun phase, the principle deformation phase related to Cretaceous crustal shortening, cannot have started before about 90 Ma at the western margin of the Upper Austroalpine nappe system (Ortler unit, Figure 22-5) because of ongoing pelagic sedimentation (Figure 22-3) up to the Cenomanian or Early Turonian (Caron et al. 1982). Thrusting further to the east and along the Schlinig thrust (basal thrust of the Oetztal unit, Figure 22-5) is constrained to have initiated earlier, at around 100 Ma, by radiometric ages of synkinematic temperature-dominated metamorphism (Thöni 1986, review of age dates in Schmid & Haas 1989). This westward migration of Cretaceous orogeny is also seen on a much larger scale across Austria, e. g. from the deposition of the synorogenic chromite-bearing Rossfeldschichten in the early Cretaceous (Faupl and Tollmann 1979) and from the pre-90-Ma age of Alpine eclogite facies metamorphism in the Saualpe (Thöni & Jagoutz 1993). This supports the postulate that continental collision along the former Hallstatt-Meliata ocean initiating during the Early Cretaceous in the eastern parts of the Austroalpine units of Austria was indeed followed by westward propagation of a thrust wedge into our area of interest by Cenomanian to Early Turonian times (Thöni & Jagoutz 1993, Neubauer 1994, Froitzheim et al. 1994).

In Figure 22-3 Cretaceous orogeny is also shown to have affected the Southern Alps (pre-Adamello phase of Brack 1981 and Schönborn 1992). The exact timing of this deformation phase is ill-constrained but certainly pre-dates

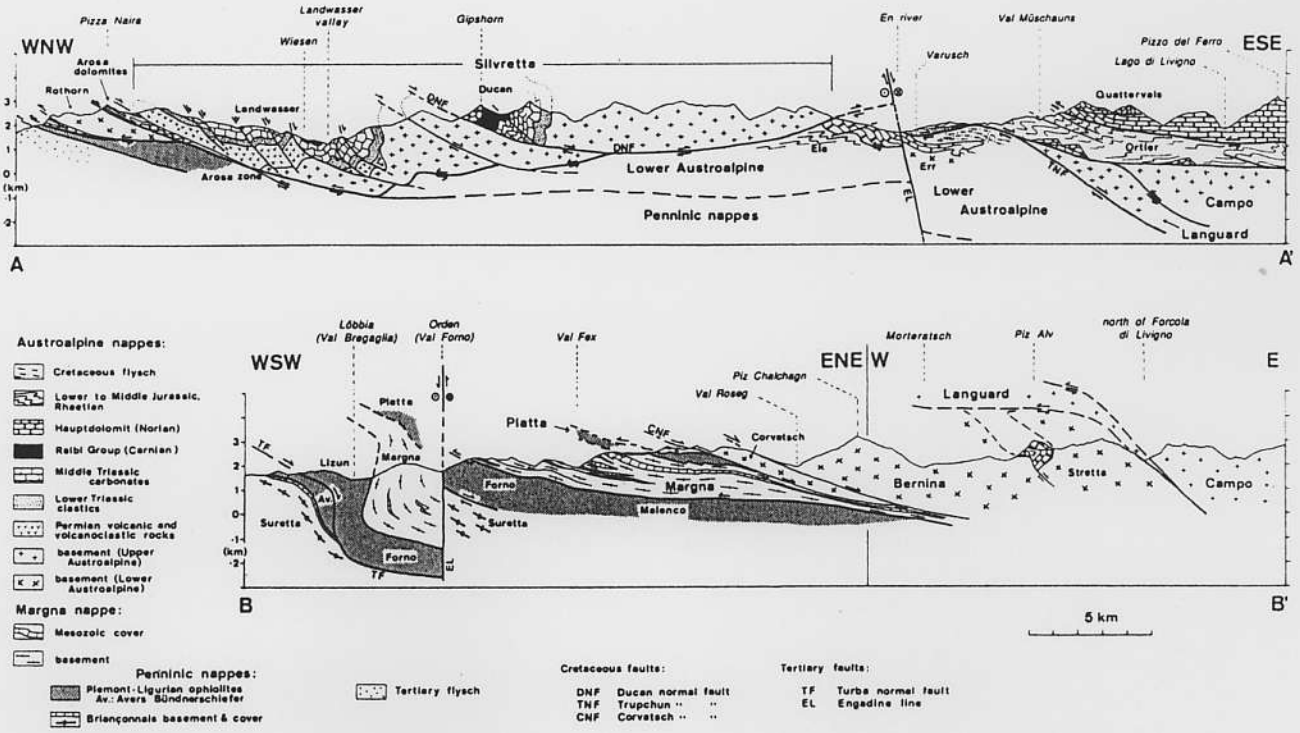

Figure 22-6
Two tectonic profiles through the Austroalpine nappes in eastern Switzerland. Profile trace indicated in Figure 22-5.

43 Ma (oldest parts of the Adamello intrusion). Assuming that flysch sedimentation in the Lombardian basin is contemporaneous with this deformation phase, and based on radiometric dating of pre-Adamello dykes crosscutting certain thrusts (Zanchi et al. 1990), a Late Cretaceous age is inferred. However, a Paleocene or Early Eocene event cannot be completely ruled out. All the top-to-the-south displacements along the Orobic thrust and parts of the displacement along the Coltignone thrust shown in Plate 22-1 are of pre-Adamello age (Schönborn 1992). This pre-Adamello N–S compression led to more than 25km of shortening and to lower greenschist facies metamorphism in the northernmost part of the Southern Alps (Orobic thrust sheet).
Activity along a precursor of the Insubric line during or immediately after Cretaceous orogeny is indicated from three lines of evidence:

(1) The kinematic and structural styles of Cretaceous deformation are totally different within the Austroalpine nappes north of the Insubric line (top-to-the-west imbrication, collision and penetrative deformation associated with metamorphism) and in the Southern Alps (top-to-the-south thrusting, foreland deformation).

(2) The Insubric line marks the limit between Cretaceous-aged metamorphic terranes to the north and the Southern Alps lacking such an overprint. Cretaceous eclogite facies metamorphism occurs in the Sesia-Dent Blanche units (Hunziker et al. 1989) and the Austroalpine units (Thöni & Jagoutz 1993), and temperature-dominated metamorphism in the Oetztal nappe (e. g. Thöni 1986). These terranes must have been at least partially exhumed by or during the Late Cretaceous and juxtaposed with the Southern Alps along this precursor of the Insubric line.

(3) The profile of Plate 22-1 directly shows a fundamental difference between the Austroalpine nappes and the Southern Alps: The former were emplaced as thin allochthonous flakes onto Penninic ophiolites in Cretaceous times, while the latter remained attached to the lower crust and upper mantle of the Apulian microcontinent, in spite of the 25km shortening of probably Cretaceous age represented by the upper crustal Orobic and Coltignone thrusts.

22.3.3 Late Cretaceous extension

Orogenic collapse behind the westward migrating Cretaceous orogenic wedge during the Ducan-Ela phase (Figure 22-3; see Froitzheim et al. 1994) led to a series of normal faults at higher tectonic levels (i. e. the normal fault at the base of the Julier nappe depicted in Plate 22-1, described by Handy et al. 1993 and several normal faults depicted in Figure 22-6, such as the Ducan, Trupchun and Corvatsch normal faults) and folding with horizontal axial planes at a lower tectonic level in the Austroalpine units of eastern Switzerland (Froitzheim 1992, Froitzheim et al. 1994). This collapse is also observed further to the east in Austria, where it is related to the formation of the 90 to 60 Ma old Gosau basins (Ratschbacher et al. 1989, Neubauer 1994). In our area of interest this extensional phase is not well dated. We place this Ducan-Ela phase somewhere between 80 Ma (end of the Trupchun phase) and 67 Ma (lower age bracket of a radiometric age determination by Tietz et al. 1993).
This Ducan-Ela phase of extension appears to have migrated westward, analogous to the previously described westward migration of the Trupchun phase. Consequently, this extension is viewed as being caused by gravitational collapse of an overthickened orogenic wedge (Platt, 1986).
Exhumation and cooling of the Austroalpine units during this Ducan-Ela phase had important implications for the Tertiary orogenic evolution of the Alps. The Austroalpine units remained largely undeformed in the Tertiary and acted as an orogenic lid in the sense of Laubscher (1983); they represented a relatively rigid block characterized by friction-controlled Coulomb behaviour floating on viscously deforming Penninic units (Merle & Guillier 1989).

22.3.4 Early Tertiary convergence and subduction (65 – 50Ma)

The tectonic evolution during Tertiary orogeny is summarized in the sketches of Figure 22-7 (see also the pioneering work along the same transect by Milnes 1987, figure 3).
The earliest possible onset of thrusting in the units below the orogenic lid formed by the Austroalpine nappes and the Platta-Arosa ophiolites (Figure 22-7a, b) is locally constrained by ongoing sedimentation in the Briançonnais domain (Paleocene in the northernmost unit of the Briançonnais, the Falknis nappe; see Allemann 1957) and in the North-Penninic Bündnerschiefer (Early Eocene in the Arblatsch and Prättigau flysch; see Eiermann 1988, Nänny 1948 and Ziegler 1956).
The sketch of Figure 22-7a represents the onset of subduction of the Briançonnais domain due to complete closure of the Piemont-Liguria ocean. The formation of an accretionary wedge within the Avers Bündnerschiefer (Piemont-Liguria ocean) and northward thrusting of this wedge onto the future Suretta nappe (southernmost Briançonnais domain) is tentatively placed in the Early Paleocene (Avers phase, Figure 22-3). This allows for continued sedimentation within most of the Briançonnais domain during the Paleocene. Onset of southernmost Briançonnais domain subduction later than 65 Ma would require convergence rates higher than 1.5 cm/yr (see Table 22-1) given the width of the paleogeographical domains adopted for constructing the

time interval	amount of convergence across the Alps	convergence rate	plate tectonic reconstruction (Dewey et al. 1989)
Early Paleocene to Early Eocene (65 - 50 Ma)	200 km inferred from relative displacement between points a and b in Figure 22-7 116 km of thinned continental crust of the Briaçonnais domain and the Valais ocean enter the cubduction zone.	1.33 cm/a	0.22 cm/a 55 Ma
			0.4 cm/a 51 Ma
Early to Late Eocene (50 - 40 Ma)	150 km inferred from relative displacement between points a and b in Figure 22-7 150 km of distal European margin situated between the southern edge of the Helvetic domain and the southern tip of stable Europe enter the subduction zone.	1.5 cm/a	1.2 cm/a 38 Ma
Late Eocone to Oligocene (40 - 32 Ma)	45 km inferred from relative displacement between points a and c in Figure 22-7 Detachment of the Helvetic sediments and deformations within the Subpenninic nappes. Unknown amount of shortening in the vicinity of the Insubric line and in the Southern Alps: 45 km represent a minimun estimate only	at least 0.55 cm/a	0.94 cm/a 19 Ma
Olifocene to Early Miocene (32 - 19 Ma)	a total of 58 km consisting of: 33 km from relative displacement between points a and c in Figure 22-7 (including 6 km out of a total ov 21 km shortening in the Aar massif) 15 km from backthrusting along the Insubric line 10 km out of a total of 56 km post-Adamello phase shortening in the Southern Alps	0.45 cm/a	
Early Miocene to recent (19 - 0 Ma)	a total of 61 km consisting of: 15 km from shortening in the Aar massif 46 km from shortening in the Southern Alps	0.3 cm/a (0.5 cm/a if deformation stopped at 7 Ma)	0.3 cm/a 9 Ma
			0.43 cm/a 0 Ma
Total time span (65 - 0 Ma)	more than 514 km	more than 0.79 cm/a	average: 0.72 cm/a amount of convergence: 481 km

Table 22-1
N–S convergence along the Eastern Traverse derived from the profiles of Figures 22-7 and plate rotation parameters of Dewey et al. (1989).

sketches (see discussion above and further discussion in Chapter 14). Such high convergence rates are unrealistic in comparison with plate movement reconstructions based on the analysis of magnetic anomalies in the Atlantic (Dewey et al. 1989). Our interpretation leaves very little time for a quiescent phase between the Cretaceous and Tertiary orogenies (the often quoted "Paleocene restoration"), somewhere near the Cretaceous-Tertiary boundary (Figure 22-3).

By the end of the Early Eocene (Figure 22-7b) the entire width of the Briançonnais domain had been subducted, together with those parts of the North-Penninic Bündnerschiefer or Valais basin that are assumed to have been underlain by oceanic lithosphere. Sedimentation in parts of the North-Penninic Bündnerschiefer basin continued up to this time (Arblatsch and Ruchberg flysch). The Tambo and Suretta nappes, representing the southern parts of the Briançonnais domain continental basement, must have reached their maximum depth (corresponding to peak pressures of 10–13kb, see Baudin and Marquer 1993) no later than this time (about 50 Ma), in order to allow for subsequent heating to peak temperatures at 40–35 Ma (discussion in Chapter 14, Hurford et al. 1989). Because the onset of penetrative cleavage formation (Ferrera phase of Figure 22-3) is associated with this metamorphism it is assumed to have started near the Paleocene-Eocene boundary in the Tambo and Suretta nappes. This significantly predates the onset of the Ferrera phase deformation in the North-Penninic Bündnerschiefer (Figure 22-3). This finding is in accordance with the general trend of northward younging for the onset of penetrative cleavage formation shown in Figure 22-3.

The northern parts of the Briançonnais basement are assumed to have been permanently subducted ("subducted Briançonnais" in Figure 22-7b). At about 50 Ma, the southern tip of stable Europe, represented by the Adula nappe, is about to enter the subduction zone. Figure 22-7b represents a snapshot of the onset of final collision caused by the complete closure of the North-Penninic Bündnerschiefer realm.

The convergence rate resulting from the relative displacement (200km) of points "a" (northern edge of the orogenic lid represented by the Austroalpine nappes) and "b" (southern tip of stable Europe, i.e. the Adula nappe) in Figures 22-7a and 22-7b is 1.3 cm per year (Table 22-1). It is noteworthy that the reconstruction of Figure 22-7 implies that the northern tip of the Austroalpine nappes marked by "a" in Figure 22-7a (and corresponding to the front of the Northern Calcareous Alps in a present-day profile, see Figure 22-7g) has moved northward by a total of about 450km relative to a point attached to stable Europe presently situated below the northern edge of the Northern Calcareous Alps. This 450 km of convergence (out of a total 514 km of Tertiary N-S convergence across the Alps, Table 22-1), was accommodated by subduction and shortening within the northern foreland. Relative to stable Europe, point "a" in the sketch of Figure 22-7a would have to have been located near Pisa in Northern Italy at the onset of Tertiary convergence. This illustrates well the important point that Cretaceous orogeny took place far from the present-day position of the Austroalpine nappes at the front of the Alps, overriding the southern Molasse basin.

22.3.5 Tertiary collision (50–35 Ma)

Collision of stable Europe with the orogenic lid led to the situation in Late Eocene times depicted in Figure 22-7c. Rapid exhumation of the Adula eclogites immediately followed and the establishment of the stack of the higher Penninic nappes occurred by the Early Oligocene (Figure 22-7d).

The amount of convergence between the stages of Figures 22-7b and 22-7c (Table 22-1) is determined by the peak depth of the Adula nappe (corresponding to 27kbar reported for the Cima Lunga unit by Heinrich 1986) and the chosen subduction angle. Other important constraints on the convergence rate are offered by the interpretation of the Adula nappe as representing the southern tip of the European foreland and the Tertiary age of eclogite facies metamorphism (Figure 22-3) inferred from geochronological (Becker 1993, Gebauer et al. 1992, 1996) and structural (Partzsch et al. 1994) data. Based on these constraints the convergence amounts to 150km, or 1.5 cm/yr. The additional 45 km of shortening inferred to have been produced between the stages illustrated in Figures 22-7c and 22-7e (indicated by the relative movement of points labelled "a" and "c", see Table 22-1 and Figure 22-7) is a minimum estimate since it does do not account for an unknown amount of retroshearing associated with the initial phases of backthrusting and vertical extrusion in the vicinity of the Insubric line.

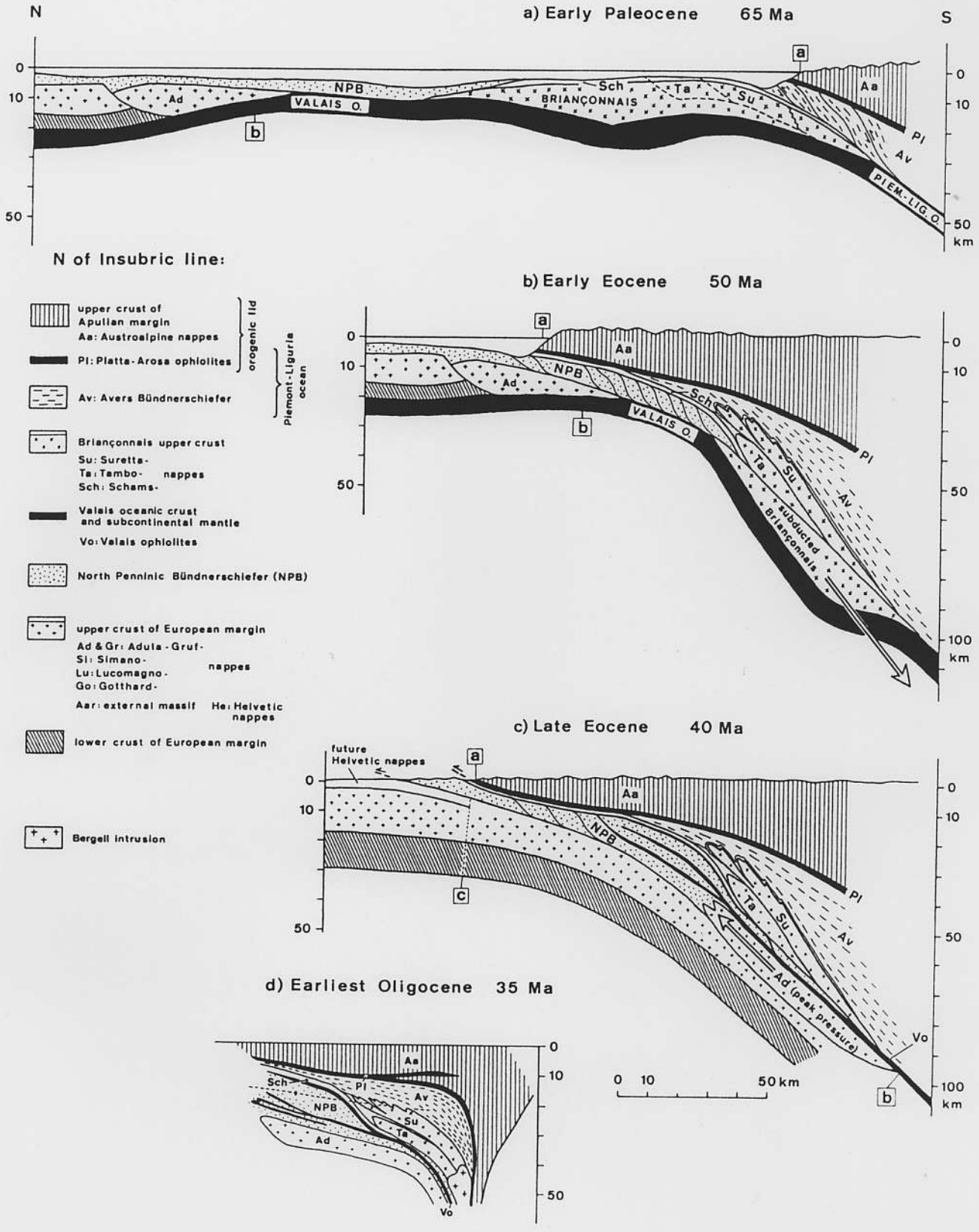

Figure 22-7
Scaled and area-balanced sketches of the kinematic evolution of the Alps from early Tertiary convergence and subduction (stages a and b) to collision (stage c) and post-collisional shortening (stages d to g).

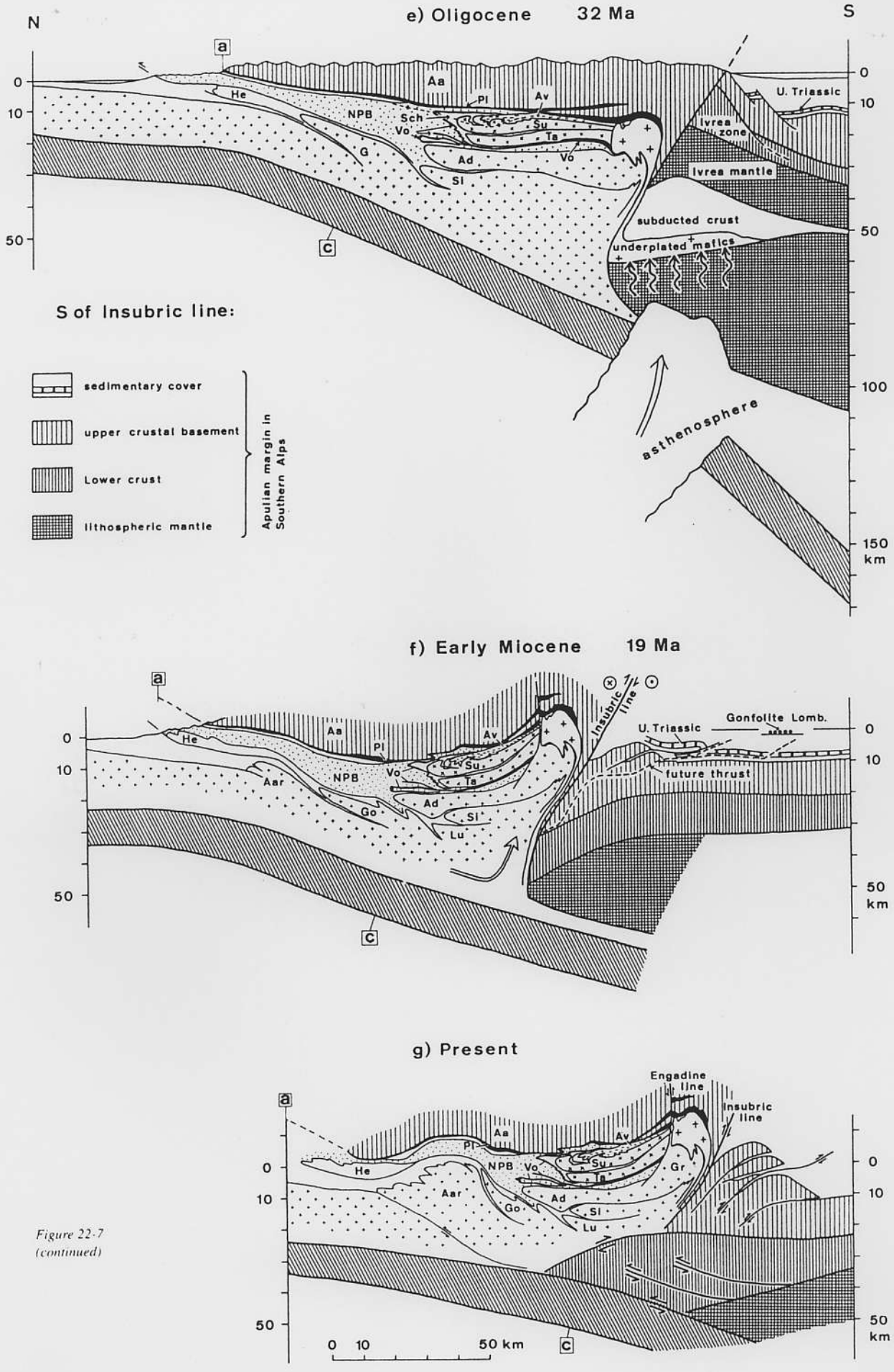

Figure 22-7 (continued)

The time span corresponding to the collisional event (50 to 35 Ma) was characterized by penetrative deformation in the Tambo, Suretta and Schams nappes (Ferrera phase of Figure 22-3). The Ferrera phase deformation within the North-Penninic Bündnerschiefer falls entirely within this time interval. Intense imbrication of Mesozoic sediments, continental basement, and mafics rocks of possibly oceanic origin within the future Adula nappe (Sorreda phase, Löw 1987) occurred under prograde conditions. This phase was followed by the Zapport phase (Löw 1987), which was characterized by extremely penetrative deformation, initially under eclogite facies conditions, followed by lower pressure metamorphic conditions arising from near isothermal decompression.

During Tertiary collision the Penninic nappes thrust northward onto the foreland, forcing the detachment of sediments that later formed the Helvetic nappes from their original substratum, i.e. the present Gotthard "massif" (D1 in Figure 22-3) at the end of the collisional stage. The age of the Tertiary cover basal unconformity (Herb 1988, Lihou 1995) in the Helvetic nappes and the internal Aar massif (Infrahelvetic units) decreases toward the foreland (Figure 22-3). This decrease may be interpreted in terms of northwestward migration of a peripheral bulge within the subducting European plate across the Helvetic realm during the Eocene. During later stages of orogeny this bulge migrated into its present-day location north of the Molasse basin (Black Forest). The northward thrusting of the Penninic units also led to a substitution of the southern Gotthard "massif" cover. The original cover, which was sheared northward to become the incipient Helvetic nappes, was replaced by Subpenninic cover slices ("Triassic, Lower, and Middle Jurassic cover slices" in the legend on Plate 22-1). This northward propagation of the basal Penninic thrust is held responsible for the detachment of North-Penninic or Ultrahelvetic (e. g. Sardona flysch) and South-Helvetic (e. g. Blattengrat unit) slivers in its footwall. These slivers were dragged over several tens of kilometers and are now found above the Helvetic nappes and, additionally, above the northern Aar massif cover immediately west of the profile of Plate 22-1 in the Glarus Alps. Emplacement of these exotic strip sheets occurred during the Pizol phase (Figure 22-3; see Milnes & Pfiffner 1977). This phase postdates the youngest sediments in the respective footwalls (Late Eocene in the Helvetic nappes, Early Oligocene in the cover of the Aar massif).

The early phases of exhumation of the Adula nappe brought the frontal parts of this unit to moderate pressures of around 6–8kb by about 35 Ma (Figure 22-7d), coincident with the onset of temperature-dominated metamorphism (so-called Lepontine metamorphism, Frey et al. 1980) in this area (Figure 22-3, see discussion in Chapter 14). This temperature-dominated metamorphism resulted from decompression along a continuous p-T loop (Löw 1987). Because the Bergell intrusion is located in direct contact above the Adula nappe (Plate 22-1) this early exhumation of the Adula nappe must have predated the intrusion. The Bergell tonalite was emplaced at a depth of merely some 20 km at its base during the Early Oligocene (pressure estimates of Reusser 1987, Davidson et al., in press). Early exhumation of the Adula nappe appears to have been extremely rapid, having occurred over a time span of only 5 Ma (between the stages represented in Figures 22-7c and 22-7d).

Such rapid exhumation by corner flow, extension or buoyancy forces (see discusssion in Chapter 14 and review by Platt 1993) is unlikely for this early phase of exhumation. Forced extrusion (recently proposed as a viable alternative model for the exhumation of the Dora Maira eclogites by Michard et al., 1993) parallel to the subduction shear zone (arrow in Figure 22-7c) seems to be the most likely mechanism for differential exhumation of the Adula nappe in respect to both higher and lower tectonic units which did not suffer eclogite facies metamorphism (see discussion in Chapter 14).

22.3.6 Post-collisional shortening (35 Ma to present)

Substantial parts of the more internal Penninic crustal units (oceanic crust, Briançonnais and distal European crust) were subducted during early stages of convergence and collision. The entire volume of upper crust in the Subpenninic nappes, representing the more proximal parts of the European crust, however, was accreted to the orogenic wedge. Excessive thickening of the orogenic wedge after the Eocene effectively "clogged" the subduction system, such that only the detached lower crust of the European foreland continued to be subducted. This led to backfolding north of, and backthrusting along the Insubric line in front of the Adriatic wedge represented by the basement of the Southern Alps (Schmid et al. 1989). This "retro-shear" meets with N-directed detachment ("pro-shear" in the sense of Beaumont et al.,1994) at the base of the Subpenninic nappes near the interface between the upper and lower crust (Figures 22-7e,f,g).

The **first step** (35 to 32 Ma) of this post-collisional shortening is represented in Figure 22-7e. In this figure the present-day portion of the Southern Alps along the transect (Plate 22-1, Figures 22-7f and 22-7g) is replaced by a profile across the Ivrea zone (after Zingg et al. 1990) in order to account for about 50km of dextral strike-slip motion along the Insubric line after Early Oligocene times (Fumasoli 1974, Schmid et al. 1987, 1989).

Also depicted in Figure 22-7e is the break-off of the subducting lower parts of the European lithosphere proposed by von Blanckenburg & Davies (1995). The subduction of light continental lithosphere during collision created extensional forces within the slab, due to opposing buoyancy forces between the deeper subducted, relatively dense lithosphere and the shallower continental lithosphere (Davies & von Blanckenburg 1995). As a result, the slab broke off. This mechanism led to heating and melting of the overriding lithospheric mantle by the upwelling asthenosphere. Melting resulted in mixing of basaltic magmas with assimilated crustal material. Such mixing is indicated by the geochemical and isotopic signatures of the Periadriatic intrusions (von Blanckenburg & Davies 1995), in particular the Bergell intrusion. Ascent and final emplacement of the Bergell intrusion are depicted in Figures 22-7d and 22-7e, based on field data by Rosenberg et al. (1994 & 1995).

The 30 and 32 Ma radiometric ages of the Bergell tonalite and granodiorite (von Blanckenburg 1992) provide excellent time constraints for dating deformation along the Insubric line and the adjacent Penninic units. Figure 22-7e depicts the situation immediately after final emplacement of this intrusion at a depth constrained by hornblende barometry (Reusser 1987, Davidson et al., in press). The Southern Steep Belt and the Insubric line must have existed prior to the ascent and final emplacement of the Bergell intrusion (Rosenberg et al. 1995). Therefore this steep zone is inferred to have formed at the Eocene-Oligocene boundary (Figures 22-3 and 22-7d). As suggested by Trümpy (1992) and Rosenberg et al. (1995) the ascent of the Bergell pluton is facilitated by movements along the Insubric fault which led to uplift of the entire southern Penninic zone relative to the Southern Alps between the stages in Figures 22-7d and 22-7e.

This differential uplift of the southern Penninic zone was probably caused by upward-directed flow in the Southern Steep Belt that was deflected into north-directed horizontal movement of the Tambo-Suretta pair (Niemet-Beverin phase of Figure 22-3, see discussions in Merle & Guillier 1989, Schmid et al. 1990, Schreurs 1990, 1993, 1995, Schmid et al., Chapter 14). This in turn resulted in the spectacular refolding of the Schams nappes and parts of the North-Penninic Bündnerschiefer around the hinge of the Niemet-Beverin fold (axial trace indicated in Figures 22-7d and 22-7e).

Movements during this Niemet-Beverin phase were contemporaneous with the closing stages of the Zapport phase in the Adula nappe, the Calanda phase in the Helvetic nappes (Pfiffner 1986) and the initiation of thrusting along the Glarus thrust (Figure 22-3). Movement of the trailing edge of the Helvetic nappes at this time, depicted in Figure 22-7e, ensured that these nappes were not affected by any significant metamorphism (these rocks now exhibit anchizonal conditions). Hence, the initial stages of movements in the vicinity of the Insubric line were contemporaneous with north-directed transport in the northern foreland. Figure 22-3 documents that this contemporaneity of "pro-" and "retro-shears" in the sense of Beaumont et al. (1994) is maintained during the later stages of post-collisional deformation throughout the Neogene.

Intrusion of the Bergell granodiorite at 30 Ma also provides a useful time mark for the end of this earliest phase of post-collisional shortening, the Niemet-Beverin phase (Figure 22-3). This phase was associated with E–W-extension (Baudin & Marquer 1993), affecting the Avers Bündnerschiefer, which were cut by an east-directed normal fault at the base of the orogenic lid (the Turba mylonite normal fault depicted in Plate 22-1; see Nievergelt et al. in press). Orogen-parallel extension resulted in substantial area reduction of the Avers Bündnerschiefer between the stages of Figures 22-7d and 22-7e.

The **second step** (32 to 19 Ma) of post-collisional shortening was dominated by backthrusting of the Central Alps over the Southern Alps along a mylonite belt associated with the Insubric line. This backthrusting, in combination with erosion, led to amazingly rapid exhumation of the Bergell area at the rate of 5mm/yr (Giger & Hurford 1989). Deposition of boulders of Bergell rocks in the Gonfolite Lombarda (mainly in the Como formation of Figure 22-3) occurred only a few million years after intrusion. Based on the cooling ages coming from the southern part of the Tambo nappe in the vicinity of this intrusion (cooling below 300°C between 21 and 25 Ma as summarized in Figure 22-3 from data in Jäger et al. 1967, Purdy & Jäger 1976, Wagner et al. 1977), exhumation of the entire Bergell area to shallow crustal depths must have been completed by about 20 Ma.

Effects of the Domleschg phase (see Chapter 14) which were contemporaneous with backthrusting along the Insubric mylonite belt (Figure 22-3) were relatively weak within the central Penninic region. The large-scale structure of this region was not substantially altered during this Domleschg phase which is characterized by a steeply S-dipping crenulation with constant vergence to the north. However, important contemporaneous movements affected the northern foreland (Figure 3). There, the main activity involved movements along the Glarus thrust (Schmid 1975) and the formation of a penetrative cleavage above and below this thrust (Calanda phase, Pfiffner 1986).

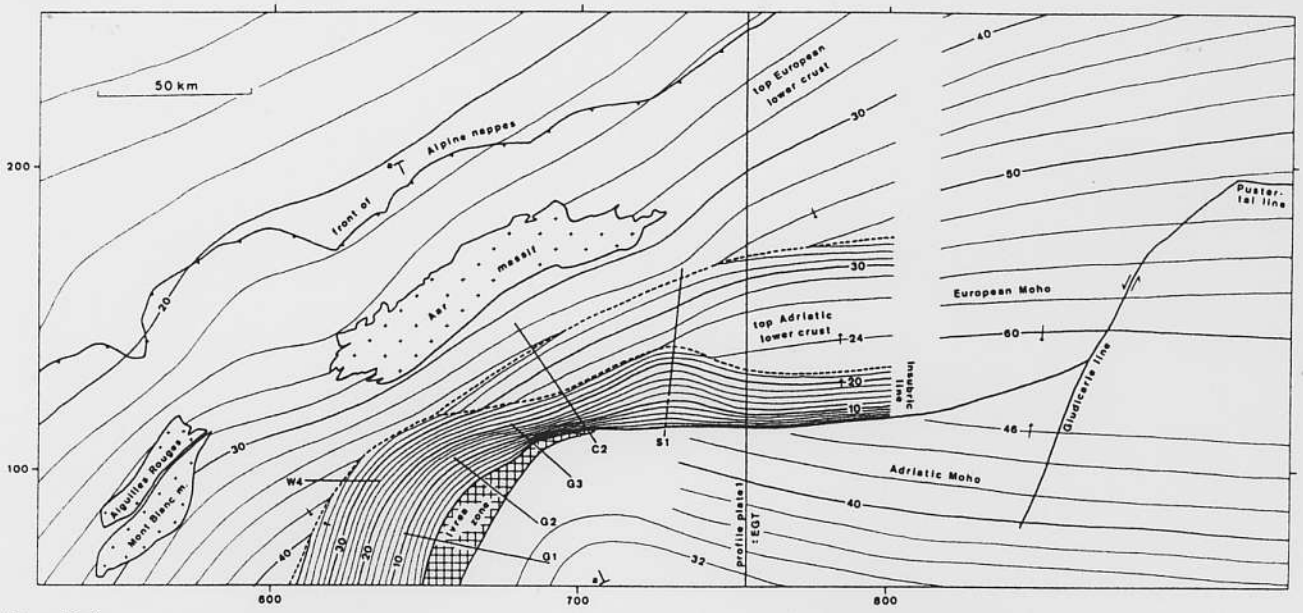

Figure 22-8

Map outlining the contours of the top of the Adriatic lower crustal wedge and its relation to the top of the European lower crust and the Insubric line, and additionally, the Adriatic and European Moho (eastern and southern part of area covered by Figure 22-8). Contour lines are given in 2 km intervals. The contours of the Insubric line are constrained by field data (Schmid et al. 1987), migrated reflection lines S1 and C2 (Valasek 1992) and 3D gravity profiles G1, G2 and G3 obtained from 3D modelling by Kissling (1980). The migrated seismic line W4 is also indicated but was not used for constraining the dip of the Insubric line. Contours of the top of the European lower crust and Moho are taken from Valasek (1992). The Adriatic Moho is contoured after data compiled by Kissling (1993) and after a seismic refraction profile by Deichmann et al. (1986). a-a: profile trace of Figure 22-9.

The leading edge of the Helvetic nappes emerged at the erosional front of the early Alps in Mid-Miocene times (Pfiffner 1986), as witnessed by Helvetic pebbles (Leupold et al. 1942) in the Upper Freshwater Molasse (OSM). The basal thrust of the Helvetic nappes (Glarus thrust in Plate 22-1) migrated towards the foreland. Displacement considerations suggest that this fault broke surface in Early Miocene times (Figure 22-7f, Pfiffner 1985). Outward migration was also true for the nappe-internal deformation (folds, thrusts, cleavage), which is attributed to the Calanda phase (Figure 22-3). This phase is of Early Oligocene age in the Helvetic nappes (Hunziker et al. 1986) and of Mid to Late Oligocene age in the internal Aar massif.

Movements at a time near the Oligocene-Miocene boundary led to the situation depicted in Figure 22-7f. These movements include: (i) dextral strike slip under brittle conditions along the Insubric line, without associated backthrusting (Schmid et al. 1989), (ii) differential uplift of the Bergell intrusion with respect to the Penninic units, caused by block rotation along the sinistral Engadine line (Schmid & Froitzheim 1993), (iii) E–W orogen-parallel extension at the eastern margin of the Lepontine dome (Forcola phase of Figure 22-3, see Chapter 14), and (iv) further movement along the Glarus thrust, leading to a second crenulation cleavage (Ruchi phase in Figure 22-3) in the area of the internal Aar massif (Pfiffner 1977, Milnes & Pfiffner 1977). Effects of contemporaneous backfolding south of the external massifs and in the northern part of the transect (Carassimo phase and formation of the Chiera synform in Figure 22-3; see Löw 1987) were relatively minor along our transect, but their importance increases rapidly further to the west. There, very intense backfolding (however of substantially younger age according to Steck & Hunziker 1994) is observed at the southern margin of the Aar massif (see Figure 22-9 and profile along the Western Traverse presented in Chapter 16). The closing stages of displacement along the Glarus thrust and the initiation of thrusting in the Molasse basin associated with shortening within the Aar massif also occurred during this second step of post-collisional deformation (Grindelwald phase in Figure 22-3; see Pfiffner et al., Chapter 13.1).

Although 33 km out of a total of 58 km shortening between the stages represented by Figures 22-7e and 22-7f took place in the northern foreland (Table 22-1), deformation in the southern part of the profile outweighted the one in the northern part during a **third step** that began in the Early Miocene (46 km out of a total of 61 km shortening, see Table 22-1). It is this final stage of post-collisional shortening that profoundly influenced the deep structure of the Alps as revealed by geophysical information, but which only led to uplift and erosion in the central part of the Alps along our transect (erosional stage of Pfiffner 1986).

According to Table 22-1 the greatest part of post-Adamello shortening in the Southern Alps occurred during this third step. It led to the impressive foreland wedge of the Southern Alps, sealed by the Messinian unconformity that formed at around 7 Ma. This post-Adamello shortening was mainly achieved by thrusting along the Milan thrust and the later out-of-sequence Lecco thrust (Plate 22-1). According to Schönborn (1992), N–S-shortening was contemporaneous and related to the displacement of the Periadriatic line by younger movements along the Giudicarie line. Retro-deformation of the post-Adamello shortening leads to a perfect alignment between the Insubric and Pustertal lines (Schönborn 1992). Together with the fact that the lower crustal volume related to this shortened upper crust is presently found at great depth north of the surface expression of the Insubric line, this is convincing evidence for a direct relationship between shortening in the Southern Alps and indentation of the Adriatic lower crustal wedge as proposed by Pfiffner (1992). Based on maps of the Moho, the Conrad discontinuity (top of the lower crust) and the top basement surface, Hitz & Pfiffner (1994) argued in favour of such a mid-crustal decoupling. Indentation of the Adriatic lower crust into the interface between the south-dipping European lower crust and the European upper crust (Subpenninic nappes) took place during this latest stage (see Figuress 7f,g and 8) and postdated final movements along the Insubric line, as already suggested by Laubscher (1990).

Shortening within the external Aar massif (Grindelwald phase of Figure 22-3) and a large part of the thrusting in the Molasse basin were contemporaneous with indentation of the Adriatic wedge (Pfiffner et al., Chapter 13.1). Outward and downward (in-sequence) propagation of thrusting also affected the Molasse basin. The depot center of this foredeep (including the Oligocene North-Helvetic Flysch deposited on the internal Aar massif) migrated outward at a rate of 0.3 cm/a in the Oligocene, slowing down to 0.2 cm/a in Miocene times (Pfiffner 1986). Thrusting in the Molasse basin and possibly folding of the Jura mountains west of our transect postdates, and in Central Switzerland actually deforms the basal thrust of the Helvetic nappes (Pfiffner et al., Chapter 13.1). Within the transect exhumation of the Aar massif from a paleo-depth of approximately 7 km to about 4 km beneath the paleo-landsurface occurred in the Miocene, as indicated by fission track data (see Chapter 13.1). The thrust indicated in Figure 22-7g at the base of the Aar massif delimits the boundary between deformed and undeformed European foreland.

Updoming of the Aar massif may be viewed as a crustal-scale ramp fold related to detachment at the interface between lower and upper European crust. This detachment is kinematically linked to the Adriatic lower crustal wedge. The intersection point between "pro"- and "retro-shears" in the sense of Beaumont et al. (1994) is now situated further to the north (i.e. at the northern tip of the lower crustal wedge) and at the interface between lower and upper European crust.

22.3.7 Plate tectonic constraints on Tertiary convergence

Amounts and rates of Tertiary convergence deduced from the kinematic reconstructions of Figure 22-7 and summarized in Table 22-1 may be compared to estimates determined from plate reconstructions. It is emphazised that the reconstructions in Figure 22-7 were determined independently of plate tectonic constraints with only one exception: the ill-dated stage represented in Figure 22-7a was placed in the lower Paleocene in order to avoid convergence rates in excess of 1.5 cm/a.

Tertiary convergence is ultimately linked to relative motions between the Eurasian and African plates. Although overall convergence rates between these two plates can be estimated (see below), many details of the smaller scale kinematics are influenced by the motion of smaller blocks or microplates such as Iberia, Apulia, Corsica-Sardinia, Mallorca and Menorca (see Dewey et al. 1989). In addition, the overall convergence is divided into shortening accommodated in the Mediterranean area and shortening in the Alpine transect studied here. As a further possibility, N–S directed extension in the Mediterranean realm may have resulted in convergence rates for the Alps that exceed the Europe-Africa convergence rate. Comparisons made below thus concern orders of magnitude and not detail.

Europe-Africa convergence rates have been analyzed on the basis of rotation parameters given by Dewey et al. (1989). The plate convergence rates were calculated between a point fixed on the northern end of the Eastern Traverse (Rorschach at +9.5° longitude and 47.5° lattitude) and a moving point on Africa (presently located in northern Libya) at the same distance from the rotation pole as Rorschach). Angular velocities for the various time intervals were determined using an average rotation pole (–15°/31°) determined from the data in Dewey et al. (1989). These velocities were then converted to local velocities (cm/a) and are listed in Table 22-1. The average velocity over the entire time span (65 Ma to present) is 0.72 cm/a, and very close to the estimate of 0.79 cm/a determined from our reconstructions. The total convergence between Europe (Rorschach) and Africa (northern Libya) is 480 km as estimated from the rotation parameters.

Local interval velocities of plate motion suggest much slower convergence rates (0.22–0.4 cm/a) in Paleocene times than the estimates based on our reconstruction (1.33 cm/a) . The reasons for this discrepancy are not clear, but might be due to independent motions of microcontinents such as the Briançonnais-Iberia terrane (Stampfli 1993). Rapid convergence (0.94 to 1.2 cm/a), however, is indicated for Eocene-Oligocene times by Dewey et al. (1989) data, in excellent agreement with our kinematic reconstruction. This higher convergence rate is linked to subduction and high-pressure metamorphism in the southern tip of Europe (Adula nappe). There is surprisingly good agreement of convergence rates in Miocene to recent times and also in respect to the total amount of convergence.

22.4 Discussion and conclusions

The Alpine section described in this contribution is similar in many ways to some of the numerical models of crustal scale deformation provided by Beaumont et al. (1994). The driving force in these models is provided by underthrusting of the mantle lithosphere (in our case the European lithosphere), coupled with asymmetric detachment emerging from a velocity discontinuity at a point (point "S") where two inclined step-up shear zones ("pro-shear" and "retro-shear") meet. The gently dipping pro-shears may be compared to the south-dipping thrust faults in the Helvetic and northern Penninic zone. More steeply inclined retro-shears, such as the Insubric line, develop above the subduction zone, causing relative uplift of the southern Pennine zone.

The analogy between model 5 of Beaumont et al. (1994), characterized by subduction of 1/3 of the crustal column, and the post-collisional stages depicted in Figures 22-7e-g is particularly striking. Intra-crustal detachment allows for simultaneous foreland migration to the north and south. Model M4 (Beaumont et al. 1994) illustrates the important role of denudation in amplifying the movement along the retro-shear. Erosion of a thickness of several kilometers of material is in fact known to have occurred in Late Oligocene times north of the Insubric line within a very short time span (Giger & Hurford 1989). This resulted in rapid exhumation of high grade metamorphic rocks north of the Insubric line (Figure 22-7e,f). Note that Figure 22-7f does not indicate the large amount of erosion which undoubtedly occurred, as documented by the deposition of Bergell boulders in the Gonfolite Lombarda of the Southern Alps.

In the course of Miocene and Pliocene times the singularity point "S" (Beaumont et al. 1994) between the pro- and retro-shear migrated northward (Figures 22-7f and 22-g). This corresponds to the tip of the Adriatic wedge encroaching along the top of the European lower crust, uplifting the Alpine nappe stack. Between 19 Ma (Early Miocene, Figure 22-7f) and 8 Ma (Mid Miocene: end of sedimentation in the Molasse basin) the tip of the Adriatic wedge migrated over a distance of about 38km (related to shortening in the Subalpine molasse and Aar massif), i.e. at a rate of 0.4–0.5 cm/a. This rate is faster than the migration of the depot center (0.2 cm/a) in the foreland basin in the same time span.

Migration of the singularity point (tip of the Adriatic wedge) during the Miocene corresponds to uplift of that part of the orogenic wedge which is located between the pro- and retro shears. The step-up of the pro-shear includes the basal thrust of the Aar massif. The retro-shear comprises the thrust fault at the top of the N-moving wedge, which links to the thrust faults in the Southern Alps (but not the Insubric line, which is inactive by this time).

Deflection of the European crust by thrust loading caused some downwarping of the pro-thrust shear zone, as well as a migration of the bulge towards the foreland (hinge retreat). Thrust loading thus created some accommodation space (Sinclair & Allen 1992) in the foredeep, which was then filled with Molasse sediments (upper USM, OMM and OSM). The fact that the migration rate of the depot center, or accommodation space, was slower than the advance rate of the singularity point, or tip of the Adriatic wedge (0.2 versus 0.4–0.5 cm/a), suggests that the orogenic wedge experienced a net crustal uplift in this time interval. The alternative explanation, whereby the accommodation space is created by an ever increasing downwarping of the foredeep, would require a change of mechanical properties of the lithosphere with time (flexural rigidity), for which there is no evidence. In summary, the closing stages of collision were marked by an orogenic wedge that underwent thickening and shortening, and net uplift and exhumation. The dynamics of the wedge were driven by asymmetric subduction of lower crust and lithospheric mantle.

The model of tectonic evolution depicted in Figure 22-7 has implications for the rheological properties of the lithosphere. Shallow-dipping upper crustal detachments, typically at depths of around 4-8km below the top of the basement, are characteristic of nappe formation in the Penninic zone during collision. The existence of such shallow detachment levels might be surprising, when compared to models of rheological stratification (e.g. Ord & Hobbs 1989). It is only feasible to associate shallow detachments with the onset of crystal plasticity in quartz, once additional overburden has been created by partial subduction to considerable depth, such as depicted for the Penninic nappes in Figure 22–7a-d. It is noteworthy that this detachment level coincides with the shallowest zone of reduced P-wave velocity typical for the European crust of the northern Alpine foreland (Mueller 1977, Mueller et al. 1980).

Substantial parts of the European and Briançonnais continental crust were subducted during the collisional stage of orogeny, in contrast to the findings of Ménard et al. (1991). During the post-collisional stage, however, the thickness of the European crust increased significantly, as more proximal parts of the European margin (underlying the Helvetic realm) entered the subduction zone. This led to the detachment of the entire upper and middle crust at the interface between lower and middle crust, a characteristic of post-collisional orogeny (Figures 22-7e–g). The European lower crust represented a layer of realtively high strength, thus pointing to a 2-layer rheology of the crust, with the high strength of the lower crust being controlled by the rheology of feldspar and/or mafic minerals. In fact model M9 of Beaumont et al. (1994) produced a lower crustal wedge very similar to that shown in Figure 22-7g. Interestingly, this model assumes a 2-layer rheology for the crust (wet quartz and wet feldspar rheologies according to Jaoul et al., 1984 and Shelton & Tullis, 1981). In order to arrive at the geometry of the Adriatic lower crustal wedge depicted in Figure 22-7g, some detachment must also have occurred above the Adriatic Moho, i.e. at the base of the lower crust.

Figures 22-8 and 22-9 address some of the 3D problems in the Alps. How far may the section depicted in Plate 22-1 be taken as representative of Alpine sections further to the east and the west (Western Switzerland, discussed in Chapters 12 and 16, ECORS-CROP profile of the Western Alps, Nicolas et al., 1990)? The contour map of Figure 22-8 indicates that the Adriatic lower crustal wedge depicted in Plate 22-1 underthrusts the Insubric line by some 45km in the east (measured between the intersection point with the N-dipping Insubric line and the tip of the wedge). This displacement drops to zero at a point northwest of the Ivrea zone. Hence, the Ivrea body, which is located to the southeast and underneath the moderately NW-dipping Insubric line represents a separate and shallower wedge that reaches the surface in the Ivrea zone. The contours of the Insubric line in Figure 22-8 have been determined from the profile of Plate 22-1 and from migrated sections of seismic lines S1 and C2 (after Valasek 1992).

Only north of the western edge of the Ivrea zone is a steep dip of 75° measured in the field (Schmid et al. 1987), whereas Kissling (1980) has modeled the Ivrea gravitational anomaly with a dip of 80° along profile G3 in Figure 22-8, where the contour spacing yields a dip of 75°. The dip becomes more gentle further to the southwest where 45° are measured according to field data, arrived at by contouring the intersection of the Insubric line with 2km of topography (Schmid et al., 1987). Section G 2 of Kissling (1980) yielded

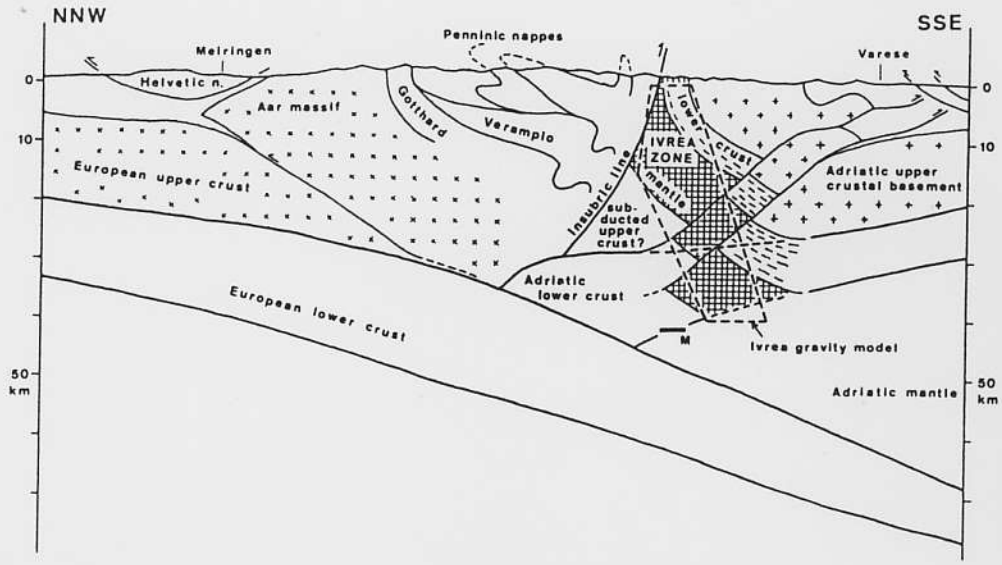

Figure 22-9
Profile west of the transect of plate 22-1 (see Figure 22-8 for location), constructed using the contours given in Figure 22-8. The position of the European Moho is taken from Valasek (1992). The Ivrea gravity model corresponds to the model of Kissling (1980, profile III). The top of the Adriatic lower crust is taken from Valasek (1992). The exact position of reflector "M" is unknown, the given approximate position is taken from Ansorge (1968).

60°, a value of 50° was assumed for constructing the contours in Figure 22-8. This angle does only slightly increase again to the southwest, where profile G1 crosses the Insubric line.

Westward decreasing indentation of the Adriatic lower crustal wedge indicates that the amount of post-Early Miocene N–S shortening within the Southern Alps (46km according to Table 22-1) also decreases towards the west. This points to the existence of a left lateral transpressive transfer zone running along the western margin of the Southern Alps (Laubscher 1991) and possibly to some counterclockwise rotation of the Southern Alps. Another left-lateral transpressive zone (the Giudicarie belt, Laubscher 1991), extending along the Giudicarie line (Figure 22-8), delimits the likely eastern termination of the Adriatic wedge. On geometrical grounds this wedge which underthrusts the Central Alps is replaced by the wedge of the Eastern Southern Alps which encompasses the entire crustal section situated south of the Tauern window (Ratschbacher et al. 1991). Note that the Giudicarie line does not appear to offset the contour lines of the European and Adriatic Moho (Figure 22-8). This is explained by the fact that the Adriatic Moho underlying the lower crustal wedge in the profile of Plate 22-1 is continuous with the Moho underlying the wedge of the eastern Southern Alps. On both sides of the Giudicarie line the Adriatic Moho overrides the uniformly S-dipping European Moho. This demonstrates the kinematic link between post-Early Miocene shortening in the Southern Alps, movements along the Giudicarie line, and north-directed indentation of the Adriatic lower crustal wedge underneath the Penninic zone (Laubscher 1990, Schönborn 1992).

The 3D problems associated with the westward termination of the Adriatic lower crustal wedge are far from solved due to incomplete seismic coverage in this area. The profile of Figure 22-9 represents an attempt to discuss some of these problems (see also Figure 11-7). In particular, a possible relationship between the Ivrea body and Adriatic lower crustal wedge is shown. Knowledge of the pre-orogenic evolution of the Ivrea zone (Schmid 1993) plays a crucial role for an improved understanding of this 3D problem. Exhumation of the Ivrea zone was related to Mesozoic passive continental margin formation near the continent-ocean transition (immediately adjacent to the Sesia extensional allochthon indicated in Figure 22-4). Alpine orogeny steepened the entire crustal section into its present-day subvertical orientation (Figure 22-9; see also Zingg et al. 1990), thereby probably exposing the ancient (Mesozoic) Moho of the Adriatic crust at the surface. This led some authors (e. g. Giese & Buness 1992) to postulate a dramatic change in the present-day topography of the Adriatic Moho near the western termination of the Ivrea zone; the northward dip of the Moho along the profile of Plate 22-1 is postulated to change into a southeasterly dip, away from the Ivrea zone and towards the west.

This direct correlation of the Paleo-Moho exposed in the Ivrea zone with the present-day Moho of the Adriatic wedge is at odds with seismic refraction data obtained along a refraction profile parallel to the Ivrea zone (Ansorge 1969). These seismic data, together with 3D gravity modelling by Kissling (1980, 1982) point to the existence of a velocity and density inversion underneath the Ivrea body and a second Adriatic Moho (labelled "M" in Figure 22-9). This second (present-day) Moho may be continuous with the north-dipping Adriatic Moho east of Figure 22-9 and beneath the transect of Plate 22-1. The cause of the density inversion below the Ivrea zone is controversial. Schmid et al. (1987) have speculated that it may be due to Cretaceous-age subduction of parts of the Sesia zone below the Ivrea body.

The contour lines of Figure 22-8 suggest that the Ivrea zone may have been underthrust by Adriatic lower crust in post-Early Miocene times. The exact geometry of the underthrust material and associated overthrust blocks within the westernmost Southern Alps is unknown and drawn schematically in Figure 22-9. This figure depicts the amount of shortening due to thrusting in this part of the Southern Alps to be substantially less (of the order of 10–20km; see also Pfiffner & Heitzmann, Chapter 11) than that further to the east (see Schumacher et al., Chapter 15, for an alternative interpretation). The geometry of the Adriatic lower crustal wedge is bound to be considerably more complex than shown in Figure 22-9.

Reconciliation of our estimate of some 500km of N-S shortening along the profile of Plate 22-1 since the Paleocene with the smaller amounts of E–W shortening recorded in the Western Alps remains a major problem, providing a challenge for future investigations. As pointed out by Laubscher (1991), large amounts of strike-slip faulting and independent motions of large blocks such as the Adriatic block were inevitable. The large amount of N–S convergence postulated along the eastern Swiss transect (Plate 22-1) indicates that much of the E–W shortening in the Western Alps must be due to an independent westward motion of the Adriatic block during the Neogene and decoupled from the Central Alps by dextral movements along the Insubric line and its precursors. There is evidence for an older and northerly directed motion in the internal zones of the Western Alps (eclogitic episode of Choukroune et al. 1986 which may have been erroneously dated as Cretaceous), suggesting that the Western Alps acted as a sinistrally transpressive belt during the Paleogene (Ricou & Siddans 1986). Only after 40 Ma did the displacement vector change into a westerly direction (Choukroune et al. 1986). Deflection of a unique west-northwest directed plate movement vector of Adria into north- and west-directed components of tectonic transport (in the Western and Central Alps, respectively) due to gravitational forces (Platt et al. 1989) is at odds with the very substantial amount of N–S convergence deduced in this study.

From the profile of Plate 22-1 the following major conclusions emerge:

1. Shortening within the Austroalpine nappes is testimony to a separate Cretaceous-age orogenic event, unrelated to the collision between Europe and Apulia that caused the closure of Penninic oceanic domains. West-directed thrusting in the Austroalpine units was related to westward propagation of a thrust wedge resulting from continental collision along the Hallstatt-Meliata ocean further to the east.

2. Considerable amounts of oceanic and continental crustal material were subducted during Tertiary orogeny, which involved some 500km of N–S convergence between Europe and Apulia. Only a very small percentage of this crustal material is preserved within the nappes depicted in the transect of Plate 22-1.

3. Post-collisional orogeny is characterized by simultaneous activity on gently dipping north-directed detachments (pro-shears) and steeply inclined south-directed detachments (retro-shears), both detachments nucleating at the interface between the lower and upper crust. This indicates a two-layer rheology of the continental crust during post-collisional orogeny.

4. Seisimic reflection and refraction information is extremely important for constraining the present-day geometry of the Alpine orogen, allowing for the reconstruction of the latest stages of orogeny. However, in view of the long-lasting history of orogeny (some 100 Ma), seismic data usually only provide a snapshot of the latest stages of this orogeny. The latest stages of orogeny in the Alps exhibit geometries that differ substantially from those of earlier stages, even given the uncertainties in the kinematic reconstructions.

Acknowledgements

We would like to thank all the numerous colleagues and students who helped in making such a compilation possible, both by their valuable research and through numerous discussions. Albert Uhr is thanked for drawing the final version of Plate 22-1 with great skill. Rudolf Trümpy and Alan Green are thanked for very carefully reviewing an earlier version of this chapter.

ALPINE CROSS SECTION ALONG THE NFP-20-EAST TRAVE

COMPILED BY S.M.SCHMID

Molasse basin and Helvetic zone by O.A.Pfiffner, Southern Alps by G.Schoenborn, Geophysics by ETH working group on Dee

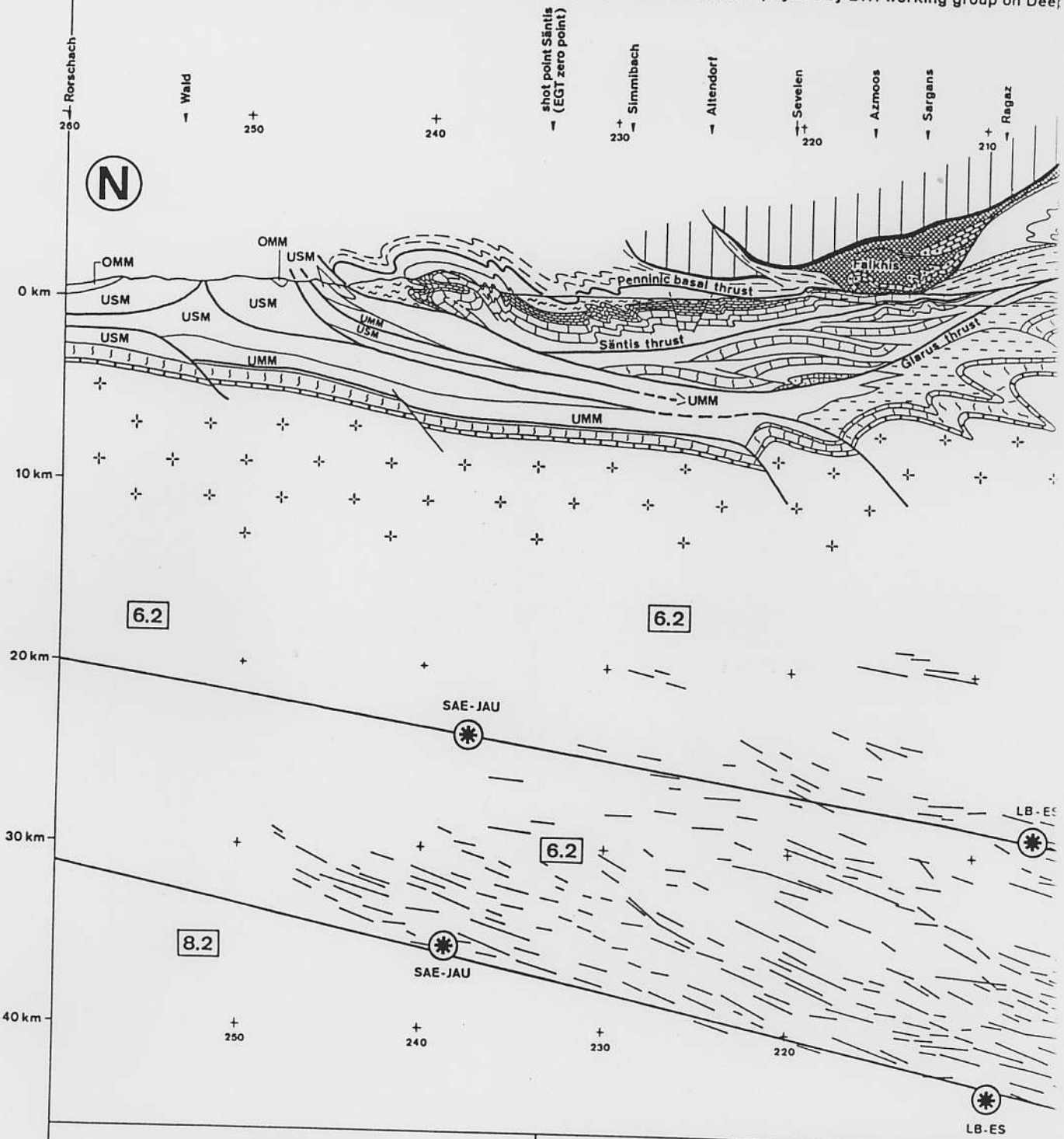

EUROPEAN MARGIN		DISTAL EUROPEAN MARGIN	VALAIS OCEAN & DISTAL EUROPEAN MARGIN	BRIA
OMM Upper Marine Molasse USM Lower Freshwater Molasse UMM Lower Marine Molasse & N. Helvetic Flysch South Helvetic slices (U.Cret. & T.) "Middle" & Upper Cretaceous Lower Cretaceous carbonates Lower Cretaceous shales Upper / Middle / Lower Jurassic Triassic Permian volcanics Verrucano Aar - Massif	Triassic, Lower & Middle Jurassic cover slices Ilanz Verrucano Gotthard "massif" Lucomago-Leventina nappes	Mesozoic, including Soja nappe Simano basement	Tertiary flysch (Arblatsch) Tomül Bündnerschiefer Tertiary flysch (Ruchberg) Grava & Prättigau Bü.-sch. Aul marble Ophiolitic slices Vals & Piz Terri Bü.-sch. Bellinzona - Dasio zone N. Adula high-p imbricates S. Adula nappe & Gruf	
HELVETIC NAPPES & N. FORELAND	SUBPENNINIC NAPPES		LOWER PENNINIC NAPPES	UPPE

OSS SECTION ALONG THE NFP-20-EAST TRAVERSE

COMPILED BY S.M.SCHMID

ic zone by O.A.Pfiffner, Southern Alps by G.Schoenborn, Geophysics by ETH working group on Deep Seismic Profiling

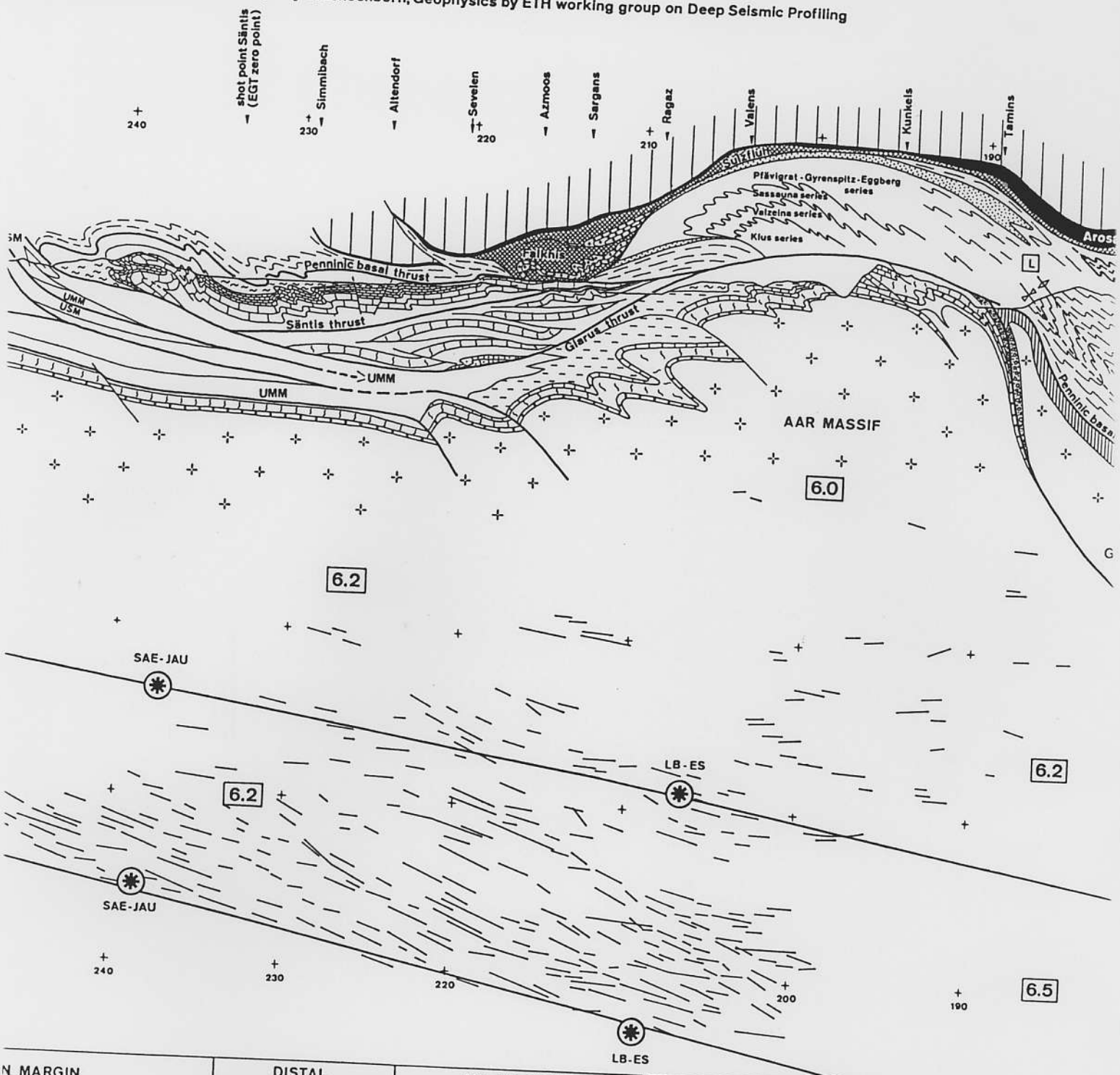

N MARGIN	DISTAL EUROPEAN MARGIN	VALAIS OCEAN & DISTAL EUROPEAN MARGIN	BRIANÇONNAIS DOMAIN
Triassic, Lower & Middle Jurassic cover slices	Mesozoic, including Soja nappe	Tertiary flysch (Arblatsch) Tomül Bündnerschiefer	Schams, Falknis & Sulzfluh Mesozoic cover nappes
Ilanz Verrucano		Tertiary flysch (Ruchberg) Grava & Prättigau Bü.-sch.	Autochthonous & parautochthonous Mesozoic cover
Gotthard "massif" Lucomago-Leventina nappes	Simano basement	Aul marble (Ophiolitic slices)	Tambo & Suretta basement
		Vals & Piz Terri Bü.-sch.	
		Bellinzona - Dasio zone	
		N. Adula high-p imbricates S. Adula nappe & Gruf	
SUBPENNINIC NAPPES		LOWER PENNINIC NAPPES	UPPER PENNINIC NAPPES

Geophysics

- Crustal model along EC
- (Y) after Ye (1992)
- (B) after Buness (1992)
- 6.2 Seismic velocities (Ye 19
- unambiguous
- doubtful

migrated as in Holli Ye (1992)

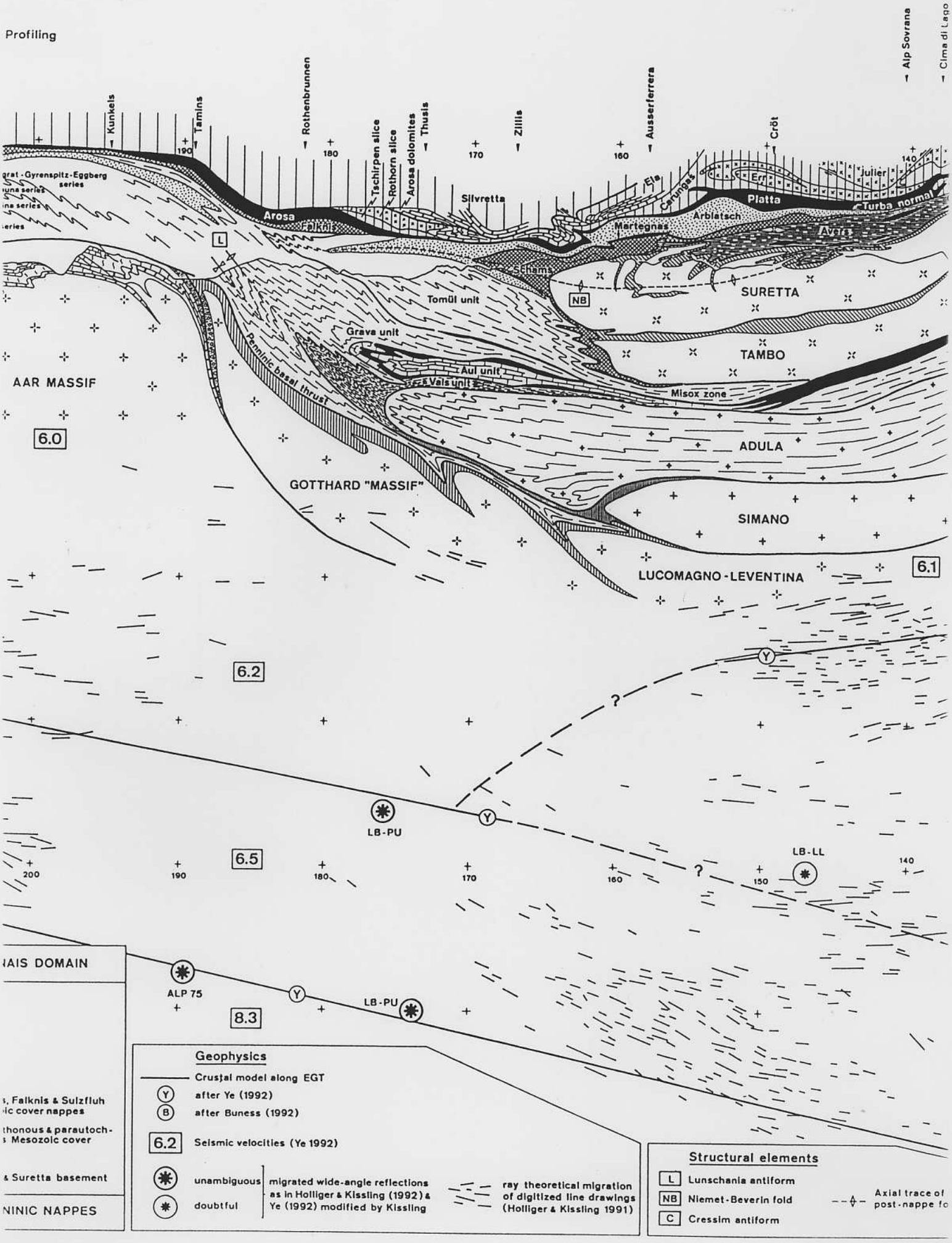
Profiling
Kunkels
Tamins
Rothenbrunnen
Tschirpen slice
Rothorn slice
Arosa dolomites
Thusis
Zillis
Ausserferrera
Crôt
Alp Sovrana
Cima di Lago
190
180
170
160
140
Julier
Err
Platta
Turba normal
Ela
Carungas
Arblatsch
Arosa
Falknis
Silvretta
Martegnas
Avers
Schams
SURETTA
NB
L
Tomül unit
Grava unit
Aul unit
Vals unit
Penninic basal thrust
TAMBO
Misox zone
AAR MASSIF
6.0
ADULA
GOTTHARD "MASSIF"
SIMANO
LUCOMAGNO-LEVENTINA
6.1
6.2
?
Y
LB-PU
6.5
LB-LL
200
190
180
170
160
150
140
ALP 75
8.3
Geophysics
Crustal model along EGT
after Ye (1992)
after Buness (1992)
6.2 Seismic velocities (Ye 1992)
unambiguous
doubtful
migrated wide-angle reflections as in Holliger & Kissling (1992) & Ye (1992) modified by Kissling
ray theoretical migration of digitized line drawings (Holliger & Kissling 1991)
Structural elements
L Lunschania antiform
NB Niemet-Beverin fold
C Cressim antiform
Axial trace of post-nappe fo
NAIS DOMAIN
s, Falknis & Sulzfluh
ic cover nappes
thonous & parautoch-
s Mesozoic cover
& Suretta basement
NINIC NAPPES

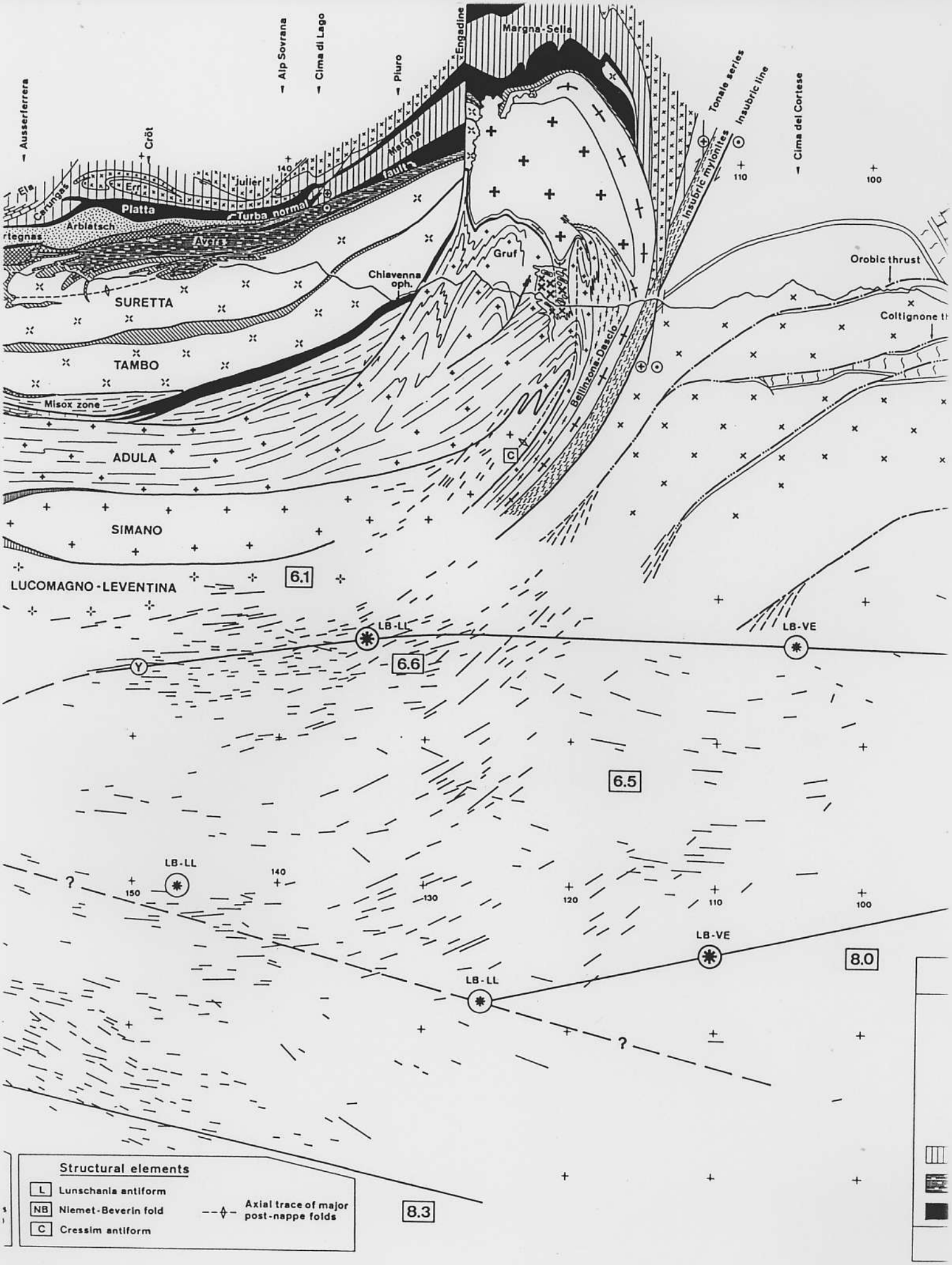
Ausserferrera
Alp Sovrana
Cima di Lago
Piuro
Engadine
Margna-Sella
Tonale series
Insubric line
Cima del Cortese
Crêt
Ela
Carungas
Err
Julier
Margna
Fault
Platta
Turba normal
Arblatsch
Avers
Gruf
Chiavenna oph.
Insubric mylonites
Orobic thrust
Coltignone
Bellinzona-Dascio
SURETTA
TAMBO
Misox zone
ADULA
SIMANO
LUCOMAGNO-LEVENTINA
6.1
6.6
6.5
8.0
8.3
LB-LL
LB-VE
C
Y
140
150
130
120
110
100
Structural elements
L Lunschania antiform
NB Niemet-Beverin fold
C Cressim antiform
Axial trace of major post-nappe folds

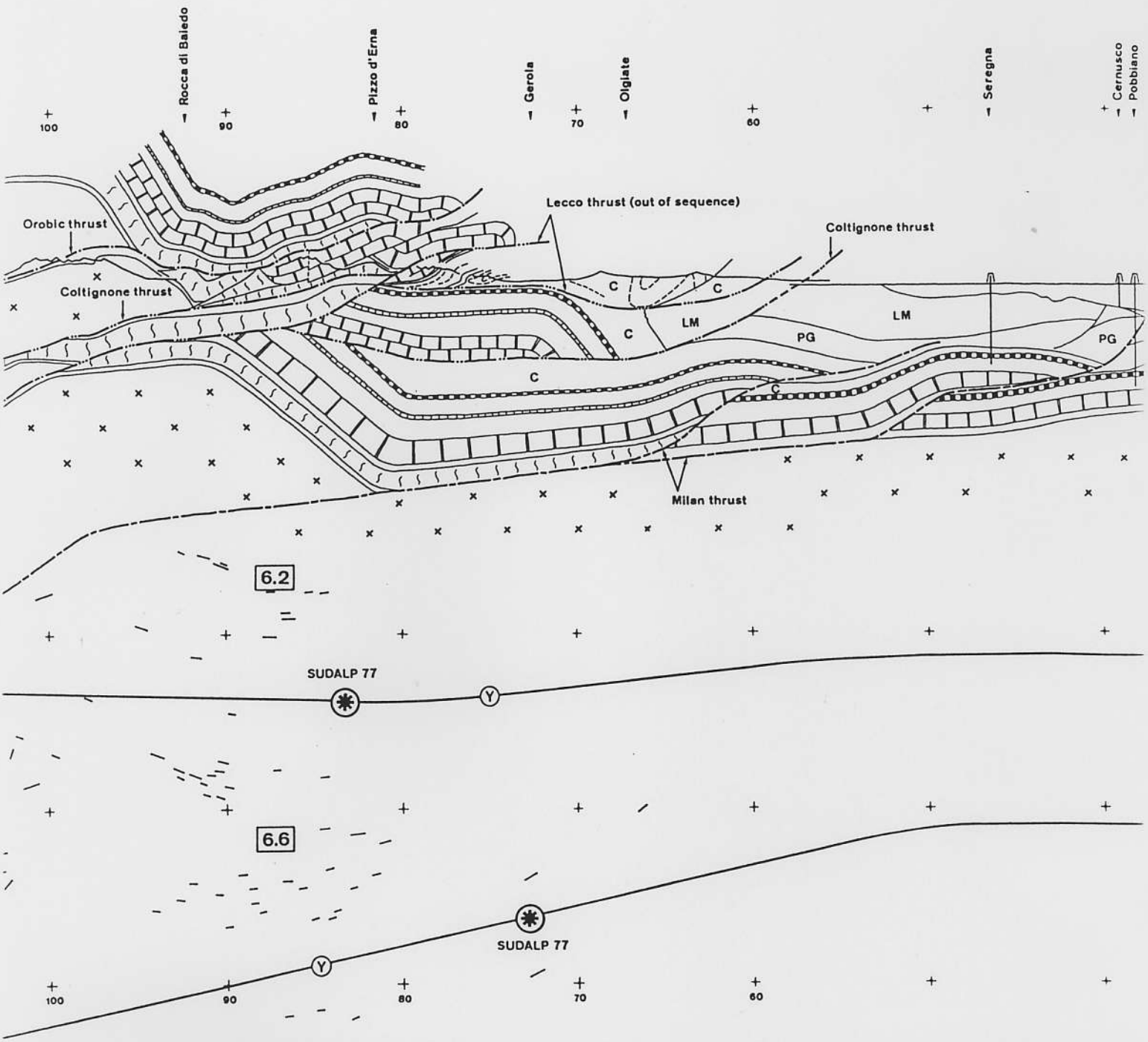

8.0

PIEMONT-LIGURIA OCEAN & DISTAL APULIAN MARGIN		APULIAN MARGIN	
Margna Sella nappes ("Ultrapenninic", Austroalpine affinities) Avers Bündnerschiefer Ophiolitic slices (Avers, Lizun, Forno, Malenco, Platta)	Novate granite post Bergell Granodiorite Tonalite Bergell intrusion (30-32 MA)	Upper Austroalpine nappes Lower Austroalpine nappes Lower Austroalpine basement	Upper Creta Paleogene (Middle Mioc Maiolica Rhaethian c Dolomia Pri Carnian Middle Tria Permian & L South-Alpin
PENNINIC-AUSTROALPINE SUTURE ZONE	TERTIARY INTRUSIONS	AUSTROALPINE NAPPES	SC

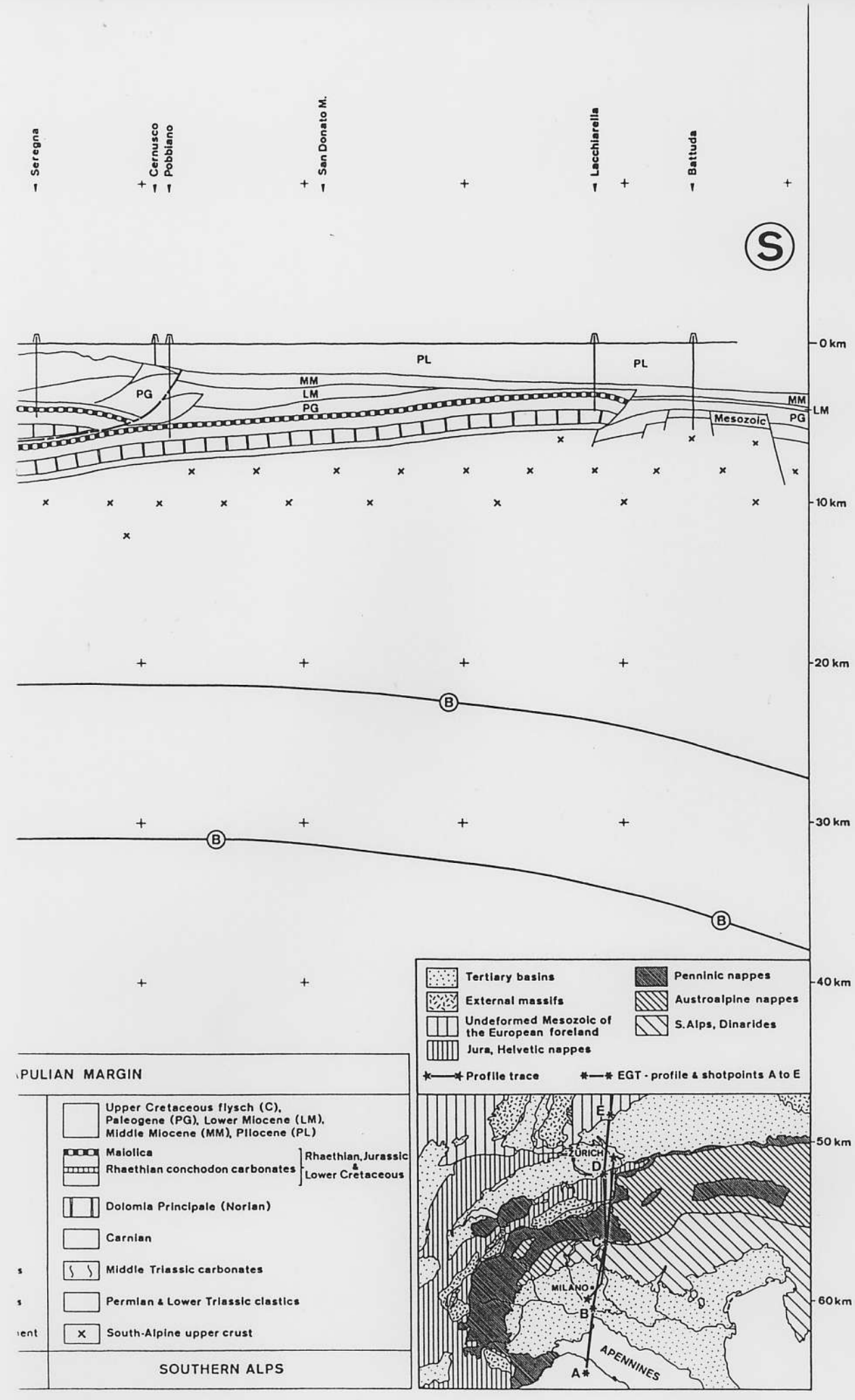
Seregna
Cernusco
Pobbiano
San Donato M.
Lacchiarella
Battuda
S
PL
PL
MM
LM
PG
PG
MM
LM
PG
Mesozoic
0 km
10 km
20 km
30 km
40 km
50 km
60 km
B
B
B
Tertiary basins
External massifs
Undeformed Mesozoic of the European foreland
Jura, Helvetic nappes
Penninic nappes
Austroalpine nappes
S. Alps, Dinarides
Profile trace
EGT - profile & shotpoints A to E
ZURICH
MILANO
APENNINES
A
B
C
D
E
APULIAN MARGIN
Upper Cretaceous flysch (C), Paleogene (PG), Lower Miocene (LM), Middle Miocene (MM), Pliocene (PL)
Maiolica
Rhaethian conchodon carbonates
Rhaethian, Jurassic & Lower Cretaceous
Dolomia Principale (Norian)
Carnian
Middle Triassic carbonates
Permian & Lower Triassic clastics
South-Alpine upper crust
SOUTHERN ALPS